Original research

Frailty subtypes and recovery in older survivors of acute respiratory failure: a pilot study

Matthew R Baldwin ,[1] Lauren R Pollack,[2] Richard A Friedman,[3] Simone P Norris,[1] Azka Javaid,[1] Max R O'Donnell,[1] Matthew J Cummings,[1] Dale M Needham ,[4,5] Elizabeth Colantuoni,[4,6] Mathew S Maurer,[7] David J Lederer [1,8]

► Additional material is published online only. To view, please visit the journal online (http://dx.doi.org/10.1136/thoraxjnl-2020-214998).

For numbered affiliations see end of article.

Correspondence to
Dr Matthew R Baldwin, Pulmonary, Allergy, and Critical Care, Columbia University, New York, NY 10032, USA; mrb45@cumc.columbia.edu

Received 8 April 2020
Revised 30 October 2020
Accepted 5 November 2020
Published Online First 9 December 2020

ABSTRACT

Background Identifying subtypes of acute respiratory failure survivors may facilitate patient selection for post-intensive care unit (ICU) follow-up clinics and trials.

Methods We conducted a single-centre prospective cohort study of 185 acute respiratory failure survivors, aged ≥65 years. We applied latent class modelling to identify frailty subtypes using frailty phenotype and cognitive impairment measurements made during the week before hospital discharge. We used Fine-Gray competing risks survival regression to test associations between frailty subtypes and recovery, defined as returning to a basic Activities of Daily Living disability count less than or equal to the pre-hospitalisation count within 6 months. We characterised subtypes by pre-ICU frailty (Clinical Frailty Scale score ≥5), the post-ICU frailty phenotype, and serum inflammatory cytokines, hormones and exosome proteomics during the week before hospital discharge.

Results We identified five frailty subtypes. The recovery rate decreased 49% across each subtype independent of age, sex, pre-existing disability, comorbidity and Acute Physiology and Chronic Health Evaluation II score (recovery rate ratio: 0.51, 95% CI 0.41 to 0.63). Post-ICU frailty phenotype prevalence increased across subtypes, but pre-ICU frailty prevalence did not. In the subtype with the slowest recovery, all had cognitive impairment. The three subtypes with the slowest recovery had higher interleukin-6 levels (p=0.03) and a higher prevalence of ≥2 deficiencies in insulin growth factor-1, dehydroepiandrostersone-sulfate, or free-testosterone (p=0.02). Exosome proteomics revealed impaired innate immunity in subtypes with slower recovery.

Conclusions Frailty subtypes varied by prehospitalisation frailty and cognitive impairment at hospital discharge. Subtypes with the slowest recovery were similarly characterised by greater systemic inflammation and more anabolic hormone deficiencies at hospital discharge.

Key messages

What is the key question?

► Can we identify clinically and biologically distinct frailty subtypes in older survivors of acute respiratory failure?

What is the bottom line?

► We identified five frailty subtypes using frailty phenotype and cognitive impairment clinical measurements made during the week before hospital discharge.

Why read on?

► Acute respiratory failure survivors are grouped into meaningfully different frailty subtypes that might help in selecting patients for post-intensive care unit follow-up clinics and clinical trials investigating novel interventions to improve survivors' recovery. Persistent systemic inflammation and multiple anabolic hormone deficiencies at hospital discharge similarly characterise several frailty subtypes with slower recovery, and may represent therapeutic targets.

INTRODUCTION

Survivors of acute respiratory failure (ARF) often have substantial disability that is acquired or worsened during the intensive care unit (ICU) stay.[1–3] Consequently, about 30% of adult ARF survivors are discharged to a postacute care facility.[1 4] Even those discharged to home have lasting physical impairment.[5–8] Studies have begun to elucidate the mechanistic underpinnings of ICU-acquired muscle atrophy and myopathy,[9–13] but the multisystem dysregulation that underlies post-ARF physical disability remains poorly understood.

Frailty is a syndrome wherein decreased reserves and dysregulation across multiple physiological systems result in functional limitations and vulnerability to new stressors.[14] Over the past decade, a majority of studies in frailty and critical care have shown that prehospitalisation frailty, measured by the clinician-assigned Clinical Frailty Scale score,[15] is independently associated with in-hospital mortality, long-term morbidity and mortality, and worse quality of life.[16] Assessing prehospitalisation frailty may help influence family discussions and clinical decision-making in the ICU. Less is known about post-ICU frailty and how it may influence mortality and physical recovery after the ICU. Discovering whether post-ICU frailty subtypes exist in ARF survivors, and investigating the potential underlying frailty mechanisms that may inhibit recovery has the potential to influence clinical care and research in ICU survivors. Specifically, identifying post-ICU frailty subtypes may inform how ARF survivors should be triaged for postacute palliative or rehabilitation care, and may help enrich

Linked

► http://dx.doi.org/10.1136/thoraxjnl-2020-216530

Check for updates

To cite: Baldwin MR, Pollack LR, Friedman RA, *et al*. *Thorax* 2021;**76**:350–359.

future post-ICU clinical trials that are aimed at improving ICU outcomes with patients most likely to have persistent post-ICU debilitation and response to rehabilitative and/or novel pharmacological interventions.

The Fried frailty phenotype (FP) domain measures of wasting, low activity, exhaustion, weakness and slowness, as well as measures of cognitive impairment capture many of the heterogeneous deficits observed in debilitated ARF survivors. We previously demonstrated the feasibility and validity of conducting a modified FP assessment in ICU survivors after the ICU, on the hospital ward, during the week before hospital discharge.[2 17] We showed that the FP, traditionally defined as deficits in ≥3 of 5 frailty domains, was independently associated with a nearly sixfold increased risk of mortality over 6 months.[17] However, we found that using the traditional cutoffs for continuous FP domain measures that were based on the lowest sex-specific quintiles of community-dwelling older adults in the Cardiovascular Health Study (CHS) were too sensitive for older ARF survivors. Seventy-three per cent of our study population was identified as phenotypically frail at hospital discharge, but we observed substantial heterogeneity in the rates of recovery in the following 6 months.

Latent class modelling was used to identify hyperinflammatory and hypoinflammatory ARDS subtypes with differential responses to higher positive end-expiratory pressure with mechanical ventilation and intravenous fluid resuscitation,[18 19] but latent class modelling has never been conducted in ARF survivors. Applying latent class modelling to FP domain measures in ARF survivors is appealing because it offers an agnostic assessment of how frailty domains may cluster in this study population.[20] Specifically, it allows measures of gait-speed, grip-strength and physical activity to be considered as continuous variables rather than categorical variables based on community-dwelling older adult population-specific lowest quintile cutoffs, and it removes the inherent measurement bias of assuming that each frailty domain measure is equally important. Given the heterogeneity of physical and cognitive deficits observed in older ARF survivors,[8] we hypothesised that a latent class analysis using FP and cognitive impairment measurements would reveal >2 clinically and biologically distinct frailty subtypes with different rates of functional recovery.

METHODS

Study design and participants

We examined ARF survivors enrolled in the Frailty and Outcomes in Critical Illness Survivors (FOCIS) study. Participants were ≥65 years old, received >24 hours invasive mechanical ventilation, non-invasive of positive pressure ventilation, or high-flow nasal cannula, and survived to hospital discharge. We enrolled only older adults (≥65 years old) because they make up the majority of adults with ARF,[4 21] because most ARF survivor cohort studies consist of predominantly middle-aged adults,[22 23] and because there remains a knowledge gap about how best to risk-stratify and identify older ICU survivors for targeted palliative, rehabilitative or therapeutic interventions. Participants were recruited from Columbia University Medical Center and the Allen Hospital, a Columbia University Medical Center-affiliated community hospital. See online supplemental E-Methods for exclusion criteria. Recruitment took place in two phases: a pilot cohort (n=22) was enrolled between February and August 2012 to ensure the feasibility of enrolling a larger cohort (n=163),[2] which was enrolled between May 2014 and June 2017. Since pilot and main cohort participants had identical inclusion/exclusion criteria and baseline study measurements, all were included in the latent class analysis. We enrolled participants and their surrogates, and obtained informed consent for both.

Clinical measurements

The baseline assessment occurred during the week before hospital discharge after participants were transferred from the ICU to the medical ward. We measured the five Fried FP domains as we have previously reported and validated.[2 17] Briefly, we measured grip-strength, gait-speed and exhaustion, and asked about weight loss in the year prior to hospitalisation using CHS methodology.[24] We assessed the physical activity domain on the basis of report of activities performed 1 month prior to hospitalisation using the Duke Activity Status Index (DASI).[25] We previously demonstrated that substitution of the DASI for the Minnesota Leisure Time Physical Activity Questionnaire,[26] the original CHS measure of physical activity, improves the construct and predictive validity of the frailty phenotype assessment in ARF survivors.[17] We used previously validated DASI score cutoffs for low activity in older ARF survivors (men ≤ 12.5; women ≤10).[17] See online supplemental E-Methods and E-Table 1 for further details. Consistent with the CHS methodology,[24] we considered participants evaluable for frailty if they had at least three measurements of the five domains, and defined the post-ICU FP as being frail in ≥3 of the five domains. We assessed for cognitive impairment at the start of the baseline assessment on the general ward. We defined cognitive impairment as either delirium (evaluated using the Confusion Assessment Method-ICU), or in those without delirium, a score ≤2 on the Mini-cog test.[27 28] We used participant/surrogate interviews and medical records to assign a Clinical Frailty Scale score based on function 1 month prior to hospitalisation, with a score ≥ 5 representing pre-ICU frailty.[15] We assessed disability as the number of basic Activities of Daily Living (ADL) disabilities 1 month prior to hospitalisation based on participant/surrogate interviews, at hospital discharge based on interviews with participants and their nurses, and at 1, 3 and 6 months during in-person or telephone interviews with participants/surrogates.[29] We ascertained the date of death from surrogates, or from national death indexes. Criteria for querying the surrogate and additional demographic and clinical variables are described in the online supplemental E-Methods.

Laboratory measurements

We obtained a blood sample on the same day as the frailty measurements. We assessed serum interleukin-6 (IL-6), tumour necrosis factor soluble receptor-1 (TNFR1), insulin growth factor-1 (IGF-1), dehydroepiandrostersone-sulfate (DHEAs), sex hormone binding globulin and albumin (see online supplemental table E2 for assay details). We measured total testosterone and 25-OH vitamin D using liquid chromatography-mass spectrometry (see online supplemental E-Methods). We calculated the free testosterone level using the Vermeulen formula.[30] We defined vitamin D deficiency as <20 ng/mL.[31] We used the lowest sex-specific study population quartile to define hormone deficiency risk groups; the conventional approach used in landmark ageing studies.[32 33] Prior to the latent class identification of frailty subtypes, 20 non-frail and 25 post-ICU FP frail participants had serum exosome isolation and enrichment, and quantitative and qualitative proteomic analyses (see online supplemental E-Methods for further details including rationale for this approach).[34]

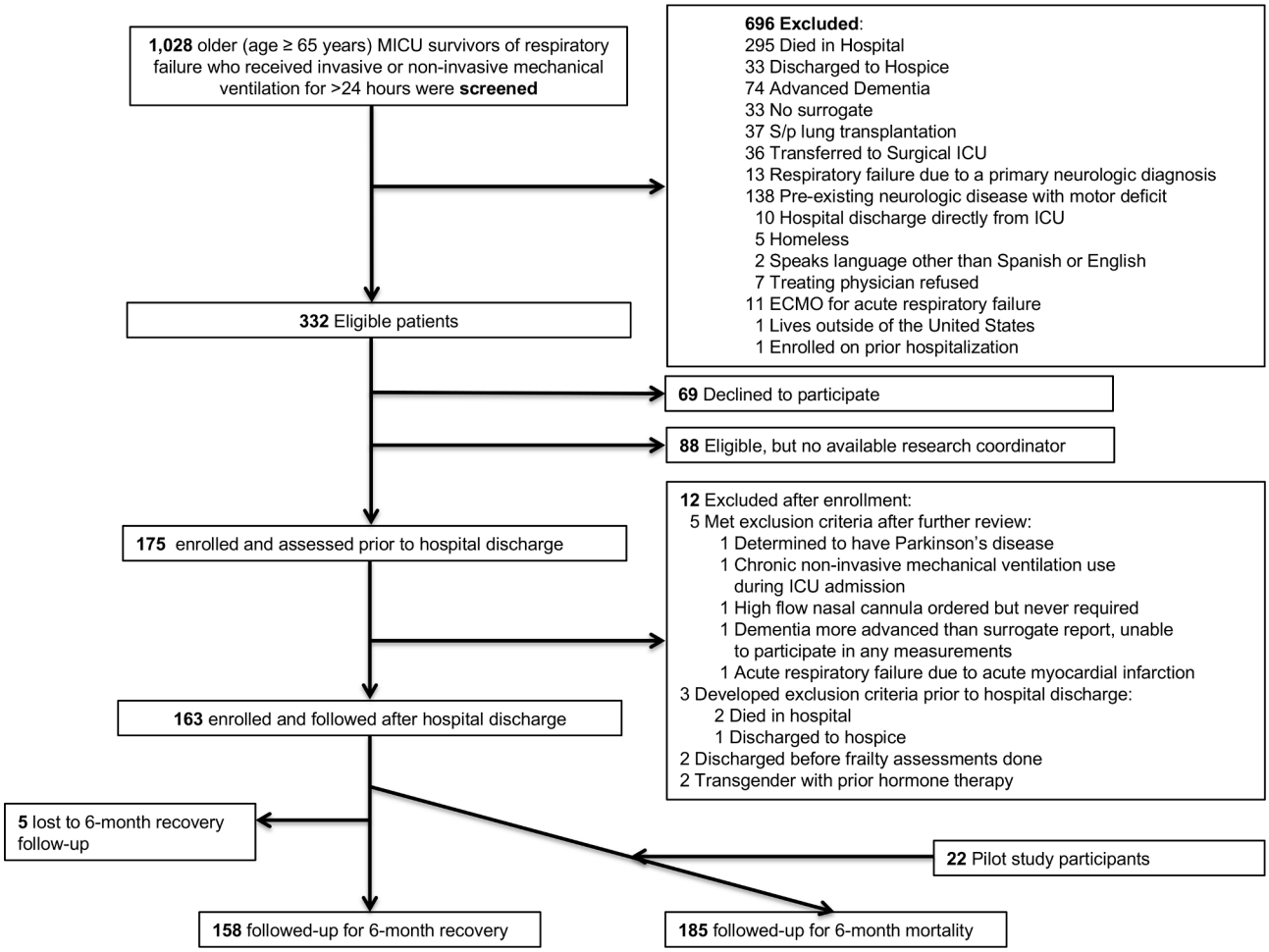

Figure 1 Study flow diagram. ECMO, extracorporeal membrane oxygenation; ICU, intensive care unit.

Latent class analysis

We conducted a latent class analysis using the five FP domain measures and the presence versus absence of cognitive impairment as latent class indicator variables. We included cognitive impairment because it is an effect modifier of the association between frailty and recovery (see online supplemental figure E1).[35] We calculated sex-specific z-scores for grip-strength, gait-speed and DASI scores. Using MPlus V.7.2 software, we fit a latent class model using the full-information maximum likelihood assumption under the missing at random assumption. We selected the optimum number of classes based on (1) the Bayesian Information Criteria (BIC); (2) Bayes Factor; (3) model entropy; (4) the size of the smallest class; and (5), the Vuong-Lo-Mendell-Rubin (VLMR) likelihood ratio test.[20] We assigned each subject to the latent class for which he/she had the maximum posterior probability.

Characterisation of frailty subtypes

We compared clinical and biomarker variables across frailty subtypes using analysis of variance, Kruskal-Wallis, χ^2, or Fisher exact tests. We assessed individual proteome-wide differential protein expression between frailty subtypes using Limma,[36] and set significance at $p<0.05$ with false discovery rate (FDR) <0.2 and an absolute $\log_2$ fold change of >0.2. We identified protein functional classes from the Reactome database of human biological pathways that differed between frailty subtypes using the Correlation Adjusted Mean Rank gene set test (CAMERA) at $p<0.05$ with FDR <0.2.[37 38] We conducted an unsupervised clustering analysis and created heat maps of differentially expressed proteins based on three groups that were found by Limma and CAMERA (subtype 1, 2 and 3–5). We identified those proteins differentially expressed by Limma which belong to the Reactome protein functional classes identified by CAMERA in order to identify which proteins may be operative in the differential protein functional classes (see online supplemental E-Methods for details).

We created Kaplan-Meier plots for survival and recovery. We defined recovery as returning to an ADL disability count $\leq$ the prehospitalisation count within 6-month follow-up. We measured time to recovery as the number of days from ICU discharge until the date of the follow-up assessment at which recovery was first achieved (ie, hospital discharge, 1-month, 3-month or 6-month follow-up). Decedents were censored at the time of death if they died prior to recovery. We excluded from recovery analyses FOCIS pilot cohort participants who never had disability follow-up, and FOCIS main cohort participants who were lost to follow-up for posthospitalisation disability assessments. We estimated the 6-month recovery rate ratio across each increasing frailty subtype using Fine-Gray competing-risks survival regression models with death as the competing risk. Models were adjusted for age, sex, pre-existing ADL disability, comorbidity, and Acute Physiology and Chronic Health Evaluation (APACHE)-II score. We confirmed the proportional hazards assumption of the Fine-Gray models using

the Schoenfeld residuals test. We conducted a sensitivity analysis to assess for time-aggregation bias due to interval follow-up after hospital discharge (see online supplemental E-Methods for details).[39]

We planned to enrol 165 participants in the main cohort, because the original goal of this study was to determine whether the post-ICU FP was independently associated with 6-month mortality.[17] At this sample size, we estimated that we would have >80% power to detect a 6-month mortality rate ratio of 1.6 per SD change in frailty score in adjusted analyses. Power cannot be directly derived for latent class models. If the sample size is too small, the number of latent class indicators too high, and the quality of the latent class indicators is too low, then latent class model non-convergence is possible,[40] which we did not observe.

RESULTS

Identification of frailty subtypes

There were 185 FOCIS participants consisting of 22 pilot and 163 main cohort participants. Frailty assessments occurred a median (IQR) 1 (0–4) days prior to hospital discharge. Five main cohort participants (3%) were lost to follow-up for disability (figure 1). Frailty domain and cognitive impairment latent class indicator variable measure missingness ranged from 0.5% to 6% (online supplemental table E3). We fit latent class models ranging from one to six classes using all 185 participants. The BIC decreased as the number of classes increased, and the Bayes Factors' were >150 for all models up to a 5-class model, providing 'very strong' evidence that the additional classes added information to the model.[41] Entropy was >0.80 in three-class to six-class models, indicating good separation of classes for these models. The smallest class size became low at 14 participants in the six-class model. Using the VLMR test, two-class, three-class and five-class models were significant improvements over models with one fewer class (table 1). We retained a final five-class model based on these results. The average latent class membership probabilities for the five-class model ranged from 0.88 to 0.95, indicating high probabilities of class assignment. We subsequently refer to latent classes as frailty subtypes.

Frailty subtype clinical characteristics

Mean (SD) ages of frailty subtypes ranged from 71 (9) years in subtype 1 to 78 (8) years in subtype 5 (table 2). Fifteen (8.1%) had chronic critical illness, defined as a tracheostomy and >10 days of mechanical ventilation.[42] Subtype 1 appeared to be clinically 'robust'. None had prehospitalisation frailty or ADL disability, they had the shortest median (IQR) ICU length of stay (2 (2–6) days, p=0.01), only 9.5% had post-ICU cognitive impairment (p=0.003), and none were post-ICU FP frail (figure 2).

Subtype 2 appeared to be 'recoverably frail'. None had prehospitalisation ADL disability, but 44% were prehospitalisation frail. They had a higher APACHE II score and longer ICU length of stay than subtype 1, 57% were post-ICU FP frail, and 20% were discharged to a skilled-care facility. Longitudinal analyses revealed a high 6-month survival and recovery to independence in ADLs (see the Frailty subtypes, survival, and recovery section).

Subtype 3 appeared to be 'acutely frail', with 26% and 89% being prehospitalisation frail and post-ICU FP frail, respectively. They had the highest APACHE II score and longest ICU length of stay among all frailty subtypes, and 63% were discharged to a skilled-care facility. Subtype 4 appeared 'chronically physically frail' with 65% being prehospitalisation frail and 93% being post-ICU FP frail, with none having cognitive impairment. Subtype 5 were 'end-stage frail' with>90% having prehospitalisation frailty, post-ICU FP frailty and cognitive impairment.

Frailty subtype biomarker characteristics

Compared with those who were robust or recoverably frail (subtypes 1 and 2), those who were acutely frail, chronically physically frail, or end-stage frail (subtypes 3–5) had higher levels of IL-6 and TNFR-1 and more vitamin D deficiency during the week prior to hospital discharge (p=0.029, p=0.039, and p=0.047, respectively; figure 3A–C). The number of anabolic hormone deficiencies in either IGF-1, DHEAs, or free testosterone increased across frailty subtypes (figure 3D). While 94% of robust patients (subtype 1) had zero or one anabolic hormone deficiencies, 45% of end-stage frail patients (subtype 5) had two or three anabolic hormone deficiencies. Patients who were deficient in all three anabolic hormones were all either acutely

Table 1 Latent class model fit statistics for one to six latent classes of frailty subtypes in older adult acute respiratory failure survivors

					Number of individuals per latent class					
Classes	BIC	Bayes factor	Entropy	VLMR p value	1	2	3	4	5	6
2	2082		0.79	<0.01	123	62				
3	2039	>2×10^{10}	0.84	0.014	96	22	67			
4	2024	1808	0.84	0.355	71	38	54	22		
5	2011	665	0.85	0.013	46	33	36	48	22	
6	2005	20	0.87	0.455	45	34	28	48	14	15

Classes	Average latent class membership probabilities					
	1	2	3	4	5	6
2	0.94	0.94				
3	0.94	0.9	0.89			
4	0.93	0.89	0.9	0.95		
5	0.88	0.95	0.91	0.88	0.95	
6	0.88	0.95	0.91	0.9	0.93	0.91

Bayes Factor compares the BIC of a model with *k* classes to the BIC of a model with *k*–1 classes. Entropy is a measure of latent class separation. VLMR likelihood ratio tests whether *k* number of classes provides improved model fit with a model using *k*–1 classes.
BIC, Bayesian Information Criterion; VLMR, Vuong-Lo-Mendell-Rubin.

Table 2 Characteristics of older adult acute respiratory failure survivors by frailty subtypes

Characteristic	All	Subtype 1	Subtype 2	Subtype 3	Subtype 4	Subtype 5	P value
Number of participants	185	21	49	35	46	34	
Demographics							
Age in years, mean (SD)	74 (8.1)	71 (8.8)	73 (7.8)	72 (6.5)	76 (8.7)	78 (7.6)	<0.001
Male	88 (48)	11 (52)	26 (53)	16 (48)	18 (39)	17 (50)	0.694
Race							0.891
White	155 (84)	19 (90)	41 (84)	29 (83)	37 (80)	29 (85)	
Black	25 (14)	1 (4.8)	6 (12)	5 (14)	8 (17)	5 (15)	
Other	5 (2.7)	1 (4.8)	2 (4.1)	1 (2.9)	1 (2.2)	0 (0)	
Hispanic ethnicity	95 (51)	11 (52)	26 (53)	23 (68)	15 (33)	20 (59)	0.037
Prehospital variables							
Residence							<0.001
Home	162 (88)	21 (100)	49 (100)	31 (89)	36 (78)	25 (73)	
Skilled-care facility	23 (12)	0 (0)	0 (0)	4 (11)	10 (22)	9 (27)	
ADL dependency count	0 (0–1)	0 (0–0)	0 (0–0)	0 (0–1)	1 (0–4)	2 (1–5)	<0.001
Clinical Frailty Scale score	4 (3–4)	2 (1–2)	4 (3–5)	3 (2–5)	6 (4–6)	6 (6–7)	<0.001
Charlson Comorbidity Index Score	2 (1–4)	1 (0–2)	2 (1–4)	3 (1–5)	3 (2–4)	3 (1–6)	<0.001
ICU variables							
APACHE II Score, mean (SD)	29 (7.8)	27 (6.5)	28 (8.1)	32 (7.7)	27 (7.5)	30 (7.4)	0.01
Type of respiratory support							0.208
Mechanical ventilation	146 (79)	18 (86)	39 (80)	31 (89)	31 (68)	27 (79)	
Non-invasive mechanical ventilation only	39 (21)	3 (14)	10 (20)	4 (11)	15 (33)	7 (21)	
ICU days	5 (3–8)	2 (2–6)	4 (3–7)	8 (4–12)	4 (2–8)	5 (3–9)	0.003
Post-ICU variables							
Post-ICU frailty phenotype score	3 (2–4)	1 (0–2)	3 (2–3)	3 (3–4)	3.5 (3–4)	4 (3–5)	<0.001
Cognitive impairment*	48 (27)	2 (9.5)	6 (13)	11 (31)	0 (0)	29 (100)	0.003
ADL dependency count at hospital discharge	4 (1–5)	0 (0–2)	1 (0–2)	5 (1–5)	5 (3–5)	6 (6–6)	0.0001
Total hospital days	12 (8–21)	9 (5–15)	11 (8–21)	16 (8–26)	13 (9–20)	14 (11–20)	0.1
Discharge location							<0.001
Home	100 (54)	19 (91)	39 (80)	13 (37)	17 (37)	12 (36)	
Long-term acute care	4 (2.2)	0 (0)	1 (2.0)	1 (2.9)	1 (2.2)	1 (2.9)	
Post acute care facility	8 (44)	2 (9.5)	9 (18)	21 (60)	28 (61)	21 (62)	
Died in 6 months	23 (15)	0 (0)	3 (7)	6 (18)	6 (16)	8 (33)	0.001

Data are presented as n (%) or median (IQR) unless otherwise stated. Cognitive impairment assessments were conducted during the baseline assessment on the ward, after the ICU, during the week before hospital discharge. Nine participants with missing cognitive impairment assessment data.
*Cognitive impaired defined as either delirium using the Confusion Assessment Method-ICU or dementia using the Mini-Cog test (score 2).
ADL, activities of daily living; APACHE, Acute Physiology and Chronic Health Evaluation; ICU, intensive care unit.

frail, chronically physically frail or end-stage frail (subtypes 3–5) (p=0.017). Serum biomarker levels are reported in online supplemental table E4.

Frailty subtype serum exosome proteomic profiles

Among the 45 participants with serum exosome proteomics, differences in demographic characteristics, clinical characteristics and recovery rates by frailty subtype were similar to those observed in the larger cohort (online supplemental table E5 and figure E2). From this sample, we identified 661 serum exosome proteins.

Differential protein expression and protein functional class analyses suggested three groups among the five frailty subtypes consisting of subtype 1, subtype 2 and subtypes 3–5. The number of differentially expressed proteins identified using Limma was greatest when subtypes 1 and 2 were compared with subtypes 3 and 5. There was little or no difference in protein expression comparing subtypes 3, 4 and 5 (figure 4A and online supplemental tables E6–14). Cluster analyses revealed that protein expression segregates to a significant although incomplete extent into groups of subtype 1, subtype 2 and subtypes 3–5 (figure 4B–D). While Limma revealed that subtype 4 had only one and four proteins differentially expressed compared with subtypes 1 and 2, respectively (figure 4A), subtype 4 still segregated mostly with subtypes 3 and 5 in cluster analyses (figure 4B–D). Using frailty subtype 1 as a comparator group, CAMERA revealed differential Reactome protein functional classes primarily related to regulation of immunity, cell replication and gene transcription, and metabolism across subtypes 2, 4,and 5 (online supplemental tables E6–9). No differential Reactome protein functional classes were identified between subtypes 1 and 3. Consistent with our protein expression findings, we did not identify any Reactome

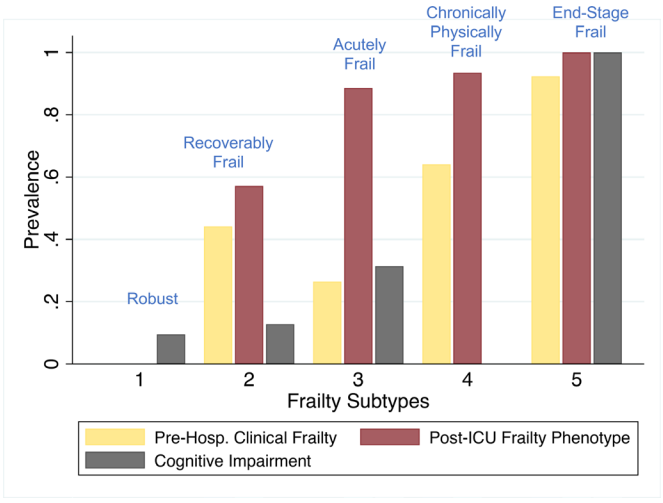

Figure 2 Prevalence of prehospitalisation frailty (Clinical Frailty Score ≥5), the postintensive care unit (ICU) frailty phenotype, and cognitive impairment (based on Confusion Assessment Method (CAM)-ICU and Mini-Cog measured during the week prior to hospital discharge) by frailty subtypes.

protein functional class differences between subtypes 3, 4, and 5 (online supplemental tables E13 and 14).

Analysis of proteins differentially expressed by Limma which belong to the Reactome protein functional classes identified by CAMERA suggest that compared with subtype 1, subtypes 2, 4, and 5 have impaired innate immunity (table 3).

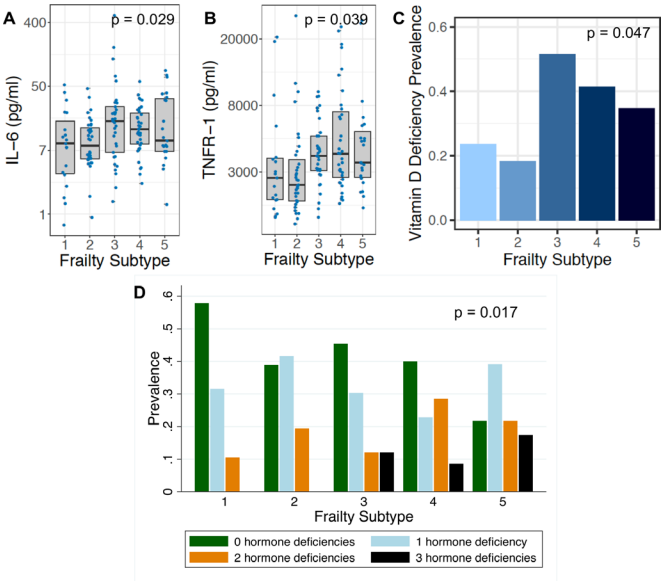

Figure 3 (A) Interleukin-6 (IL-6) and (B) tumour necrosis factor-alpha receptor (TNFR)–1 levels during the week prior to hospital discharge by frailty subtypes. Bars represent median levels, boxes represent IQR, and dots represent individual observations. (C) Prevalence of 25-hydroxy vitamin D deficiency during the week prior to hospital discharge by frailty subtypes. Vitamin D deficiency is defined as<20 ng/mL. (D) Prevalence of the number of hormone deficiencies in either insulin growth factor-1, dehydroepiandrosterone-sulfate, or free testosterone. Hormone deficiency cutoffs were defined as the sex-specific lowest quartile of the study population.

Frailty subtypes, survival and recovery

The unadjusted 6-month survival and basic ADL recovery rates both decreased significantly across increasing frailty subtypes (figure 5). All robust patients (subtype 1) survived and recovered. Among recoverably frail patients (subtype 2), 93% survived and 83% recovered. Acutely frail and chronically physically frail patients (subtypes 3 and 4) had similar 6-month survival and recovery of approximately 80% and 60%, respectively. Among end-stage frail patients (subtype 5), only 67% survived and 45% recovered. In adjusted analyses, there was an additional 42% increase in the 6-month mortality rate across each increasing frailty subtype (adjusted-mortality rate ratio: 1.42, 95% CI 1.03 to 1.94). In adjusted Fine-Gray competing-risk regression analyses, there was an additional 49% decrease in the 6-month ADL recovery rate with each increasing frailty subtype (adjusted recovery rate ratio: 0.51, 95% CI 0.41 to 0.63). Recovery rate ratio effect estimates were nearly identical in the sensitivity analysis (adjusted recovery rate ratio: 0.50, 95% CI 0.40 to 0.63), suggesting that there is no significant time-aggregation bias.

DISCUSSION

Using ARF as a model of accelerated ageing, we applied the geriatric construct of frailty to elucidate five new and meaningfully different subtypes of older ARF survivors. The acutely frail subtype has minimal prehospitalisation frailty and disability and predominantly ICU-acquired frailty and slow recovery, and therefore may be an optimal group for post-ICU physical rehabilitation. The end-stage frail subtype has pre-ICU frailty, post-ICU FP frailty, cognitive impairment, the slowest recovery rate and a 33% 6-month mortality, suggesting that they may benefit from post-ICU palliative care interventions. Frailty subtypes appear phenotypically different based on the degree of their prehospitalisation multimorbidity that is captured with the Clinical Frailty Scale, and post-ICU cognitive impairment. However, the three subtypes with the slowest recovery appear endotypically similar with persistent inflammation, multiple anabolic hormone deficiencies, and impaired innate immunity. While these deficits have been individually reported in adults with acute and protracted critical illness,[43–49] our finding of such profound inflammation and multiple anabolic hormone deficiency that persists after the resolution of critical illness in older adults preparing for hospital discharge suggests that these deficits may be clinically important and potential therapeutic targets in a much larger population of ICU survivors than previously recognised.

Previous frailty research in critical care has focused primarily on identifying prehospitalisation frailty as a risk factor for adverse outcomes.[16 50] The mechanistic underpinnings of frailty in critical care patients has not yet been thoroughly investigated. Since most critical illness is unpredictable, it has not been feasible to enrol patients and make clinical or biological measurements prior to their ICU admission. Our study advances frailty research in critical care by being the first to link clinical measures of frailty with inflammation and anabolic hormone deficiencies, common mechanisms governing age-related frailty that are driven to extreme levels by critical illness, and that might underlie the pathobiology of frailty-related physical impairment after ARF. To do this, we focused on ICU survivors; we performed frailty assessments on the medical ward near the time of hospital discharge when delirium or cognitive function may be milder, which in turn, allowed us to make measures of grip strength and gait speed[2]; and we estimated the 1-month prehospitalisation Duke Activity Status Index as the frailty domain of physical activity.[17]

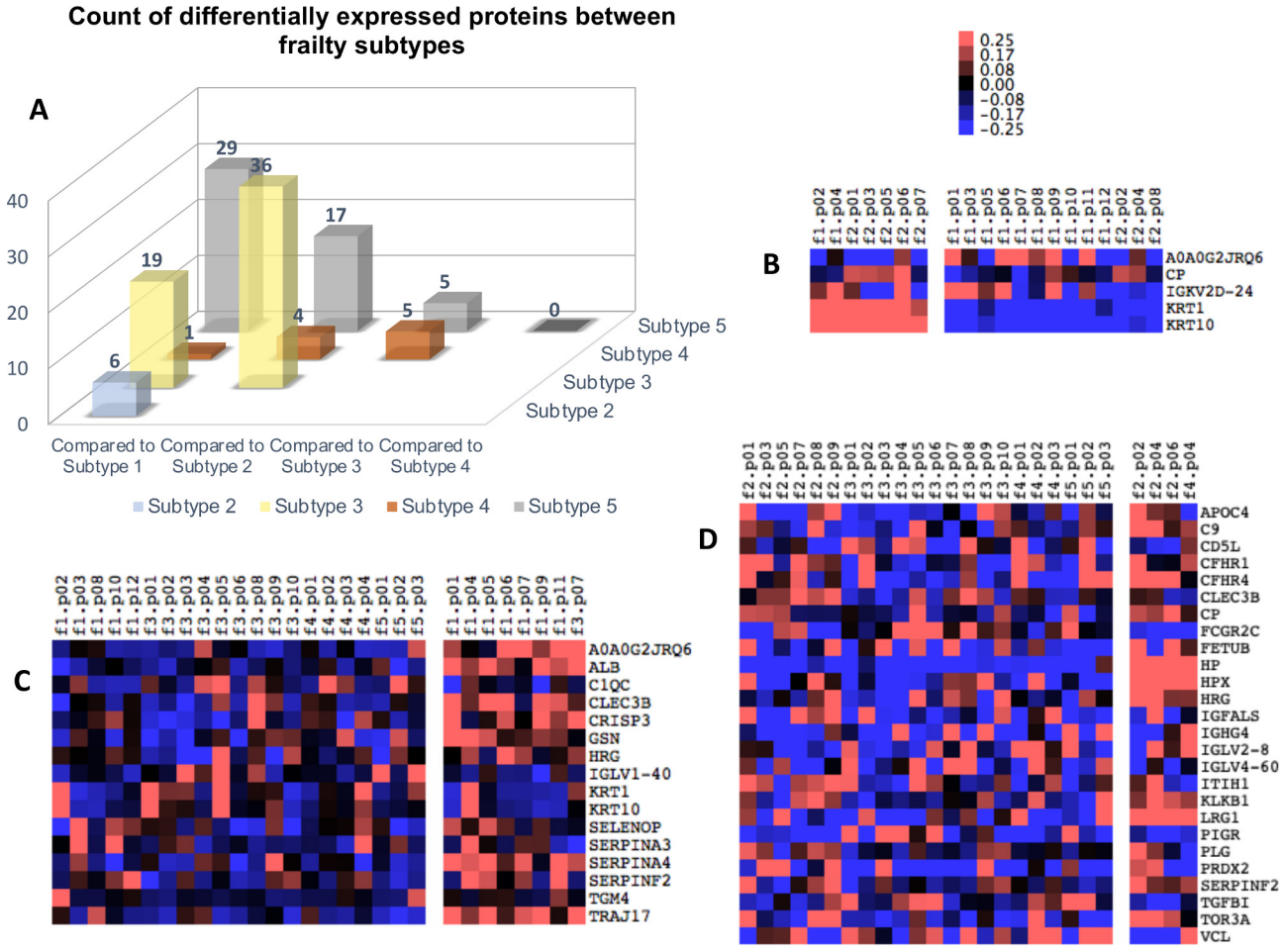

Figure 4 (A) Count of differentially expressed proteins between frailty subtypes using Limma at p<0.05 with FDR<0.2 and an absolute $\log_2$ fold change of >0.2. Specific protein names are listed in online supplemental table E6–14. Heatmaps of unsupervised cluster analyses of differentially expressed proteins between (B) frailty subtypes 1 versus 2, (C) frailty subtypes 1 versus 3–5, and (D) frailty subtypes 2 versus 3–5. Numbers in the colour legend represent $\log_2$ concentration (scale arbitrary), mean centred by protein. Individual patients are listed in columns with f# denoting the frailty subtype number and p# representing patient study identification number. Names of differentially expressed proteins are listed in the rows. Heatmaps suggest that there is significant although incomplete segregation of protein expression into three groups consisting of subtype 1, subtype 2 and subtype 3–5.

Accordingly, our measure of post-ICU frailty represents the cumulative effects of deficits that were present prior to critical illness and those acquired during critical illness.

Our finding of greater inflammation at hospital discharge in frailty subtypes with slower recovery supports the hypothesis that critical illness leads to persistent inflammation, immunosuppression and catabolic syndrome in many ICU survivors, not just those with chronic critical illness.[51] Our findings are consistent with studies that identified associations between inflammation at hospital discharge and increased 1-year mortality in pneumonia survivors,[52] and inflammation at 3 months after ICU hospitalisation and worse mobility in ARF survivors.[47] Since we measured inflammation just prior to hospital discharge, we cannot discriminate between prehospitalisation inflammation related to pre-existing frailty and persistent inflammation due to ARF. However, the mean (SD) IL-6 level among study participants was 23 (46) pg/mL, which is 5–10 times greater than in frail community-dwelling older adults.[24 53 54] Therefore, we expect that most inflammation observed in ARF survivors stems from critical illness.

Table 3 Serum exosome proteins differentially expressed that belong to Reactome functional protein classes identified by CAMERA

	Subtype 1 versus 2	Subtype 1 versus 3	Subtype 1 versus 4	Subtype 1 versus 5
Differentially expressed proteins	KRT1	No Reactome classes identified to compared with differentially expressed proteins	IGKV4-1	CLU, CRP, C4B, LCN2, TF
Reactome protein functional classes identified with CAMERA (direction of regulation)	Innate immune system (*down*)	No Reactome classes identified	Triggering of complement (*down*), creation of C4 and C2 activators (*down*)	Complement cascade (*down*), cytokine signalling in immune system (*up*), membrane trafficking (*up*)

CAMERA, Correlation Adjusted Mean Rank gene set test.

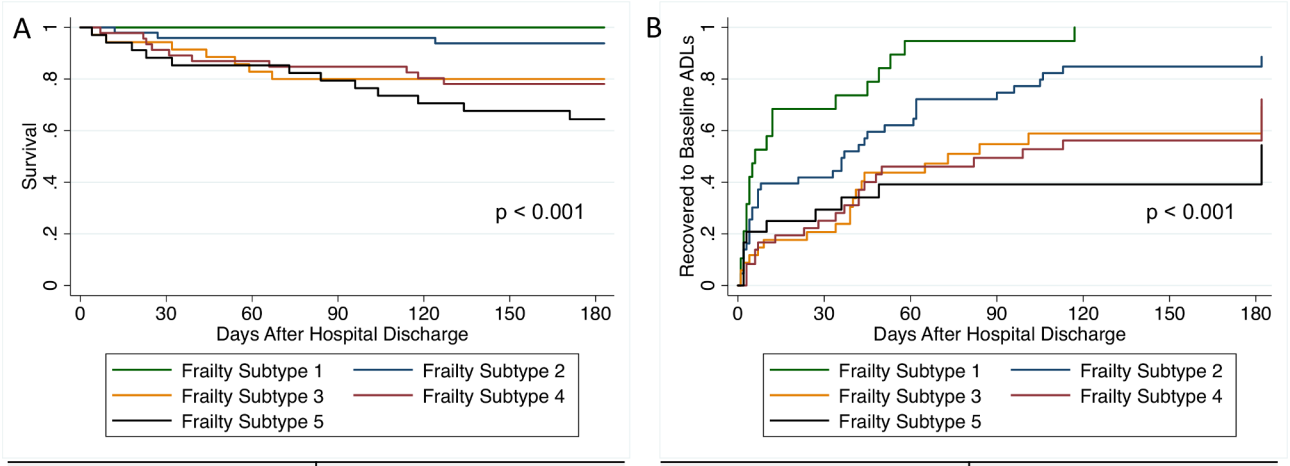

	Adjusted-Mortality Rate Ratio (95% CI)
Increasing Frailty Subtype, Reference: Subtype 1	1.42 (1.03-1.94)

	Adjusted-Recovery Rate Ratio (95% CI)
Increasing Frailty Subtype, Reference: Subtype 1	0.51 (0.41-0.63)

Figure 5 (A) Kaplan-Meier survival function plot of frailty subtypes, showing 6-month survival from hospital discharge. Mortality rate ratios are HRs estimated from Cox proportional hazards models. (B) Kaplan-Meier failure function plot of frailty subtypes showing recovery to prehospitalisation basic activities of daily living (ADLs) independence within 6 months after hospital discharge. Recovery rate ratios are estimated from Fine-Gray survival regression models. Mortality ratio ratios and recovery rate ratios are adjusted for age, sex, pre-existing ADL disability, Charlson Comorbidity Index score, and Acute Physiology and Chronic Health Evaluation II score.

Three landmark case series of prolonged mechanical ventilation patients have shown depression of the neuroendocrine axes during the ICU stay.[43–45] Our finding of multiple anabolic hormone deficiencies in a large proportion of older adult ARF survivors just prior to hospital discharge suggests that post-critical illness anabolic hormone suppression, whether pre-existing and/or ICU acquired, may be more widespread, severe and persistent than previously recognised. In community-dwelling older adults, the number of anabolic hormone deficiencies in free-testosterone, DHEA and IGF-1 predict frailty and mortality better than any single anabolic hormone deficiency,[32 55] which has led investigators to propose multiple low-dose anabolic hormone replacement therapy for frail older adults.[33 56] Since we observed multiple anabolic hormone deficiencies in frailty subtypes with the slowest recovery, future studies should investigate whether multiple anabolic hormone deficiencies after critical illness represent a therapeutic target for improving physical recovery. While our sex-specific lowest study population quartile definition for anabolic hormone deficiency follows the approach used in landmark ageing studies,[32 33] it is arguably arbitrary. However, these lowest quartile levels are lower than deficiency levels defined for adults in the outpatient setting. Applying the DHEAs cut-off of <15th percentile for young men and women that was used in a landmark DHEA supplementation trial of older adults,[57] 98% of men and 100% of women in our study would be deficient. Applying the LCMS-derived total testosterone cut-off for symptomatic hypogonadism in older men of <3.2 ng/mL,[58] 83% of men in our study would be deficient. Applying the <2.5th age-adjusted and sex-adjusted percentile for IGF-1,[59] a cut-off used to identify growth hormone deficient patients,[60] 27% of men and 20% of women in our study would be deficient.

Our study has additional limitations. Our results need to be externally validated in a cohort that also includes younger adult ARF survivors. While we excluded those with severe dementia, our measures of cognitive impairment after the ICU cannot differentiate more mild pre-existing cognitive impairment from ICU-acquired cognitive impairment. Furthermore, the Mini-cog does not pedict long-term cognitive impairment in ARDS survivors.[61] Future studies should use more robust measures of cognitive function, such as those used in the ALTOS or BRAIN-ICU cohort studies,[62 63] which may allow for better discrimination of subtypes. Our assessment of physical activity in the month prior to hospitalisation is susceptible to mismeasurement. However, other studies support that recall and surrogate response bias of physical activity in ICU survivors is minimal,[64–66] and we previously showed that the DASI has high construct and predictive validity in ARF survivors.[17] We estimated mortality and recovery rate ratios for each increasing frailty subtype while controlling for severity of illness with the APACHE-II score, but we did not control for daily sequential organ failure assessment scores. We assessed serum exosome proteomics because prior frailty-related plasma proteomic profiling in community-dwelling older adults was unrevealing,[67] and because serum exosomes are involved in relevant pathobiological functions of organs affected by critical illness stressors.[68] However, serum exosome proteomic profiling remains a new field, and our results should be considered exploratory. Recent advances in plasma proteomic profiling techniques have led to identification of plasma proteomic signatures of age in healthy humans.[69] Therefore, using plasma proteomics to assess multisystemic dysregulation in ARF survivors should be reconsidered. We did not assess for impaired muscle mitochondrial bioenergetics, an additional mechanism of age-related frailty that has been implicated in ICU-acquired weakness.[70–72]

In summary, we identified five different frailty subtypes, that if validated, could help identify patient subgroups that may maximally benefit from targeted post-ICU rehabilitation or palliative care. Combined physical and cognitive rehabilitation, which has been shown to be feasible in ICU survivors,[73] could be considered in those subtype patients who have both new disability and cognitive impairment at hospital discharge. Consistent with complexity underlying frailty, no single biological frailty deficit appears to dominate any single frailty subtype. Instead, multiple frailty subtypes with the slowest recovery and highest mortality

all appear to have a combination of persistent inflammation, multiple anabolic hormone deficiencies and immunosuppression. Our observation that an acutely frail ARF survivor subtype appears to have inflammation and anabolic hormone deficiencies at hospital discharge similar to subtypes with chronic physical frailty or end-stage frailty supports the hypothesis that the critical illness of ARF accelerates age-related frailty mechanisms in older adults. Our findings suggest that a systems biology approach to further understand the multisystemic dysregulation that persists after ARF may be very revealing and supports the hypothesis that post-ICU therapeutic interventions may need to target multiple deficits simultaneously in order to successfully improve recovery after critical illness.

Author affiliations
[1]Pulmonary, Allergy, and Critical Care, Columbia University Irving Medical Center, New York, New York, USA
[2]Medicine, University of Washington School of Medicine, Seattle, Washington, USA
[3]Bioinformatics, Columbia University Irving Medical Center, New York, New York, USA
[4]Outcomes After Critical Illness and Surgery Group, Johns Hopkins University, Baltimore, Maryland, USA
[5]Division of Pulmonary and Critical Care Medicine, Johns Hopkins University School of Medicine, Baltimore, Maryland, USA
[6]Department of Biostatistics, Johns Hopkins University—Bloomberg School of Public Health, Baltimore, Maryland, USA
[7]Cardiology, Columbia University Irving Medical Center, New York, New York, USA
[8]Regeneron Pharmaceuticals, Tarrytown, New York, USA

Twitter David J Lederer @davidlederer

Acknowledgements The authors are grateful to Wendy C Gonzalez, research coordinator for the Frailty Outcomes in Critical Illness Study, who helped recruit and follow-up the majority of participants in this study.

Contributors MRB, MSM and DJL conceived of the study and its design. MRB had full access to the data. MRB, RAF and EC take responsibility for the integrity of the data and accuracy of the analysis. MRB, LRP, SPN and AJ organised and entered data. MRB, LRP, SPN, AJ, MRO, MJC, DMN, EC and DJL contributed to data analyses. MRB, LRP, RAF, MRO, MJC, DMN, EC, MSM and DJL contributed to data interpretation. MRB drafted the manuscript. All authors critically revised the drafted manuscript and approve of the submitted manuscript.

Funding MRB is supported by NIH grant K23 AG045660, a faculty research fellowship from the Columbia University Ageing Centre, and the Columbia University Irving Institute (NIH grant UL1 TR001873). DJL was supported by NIH grants R01 HL103676, R01 HL137234 and K24 HL131937. MSM was supported by NIH grant K24 AG036778.

Competing interests None declared.

Patient consent for publication Not required.

Ethics approval The Columbia University institutional review board approved this study (protocols AAAI1864 and AAAN7107).

Provenance and peer review Not commissioned; externally peer reviewed.

Data availability statement Data are available upon reasonable request. Deidentified participant data are available from MRB, MD, MS ORCID: https://orcid.org/0000-0003-4670-3433.

ORCID iDs
Matthew R Baldwin http://orcid.org/0000-0003-4670-3433
Dale M Needham http://orcid.org/0000-0002-9538-0557
David J Lederer http://orcid.org/0000-0001-5258-0228

REFERENCES

1 Wunsch H, Guerra C, Barnato AE, *et al*. Three-year outcomes for Medicare beneficiaries who survive intensive care. *JAMA* 2010;303:849–56.
2 Baldwin MR, Reid MC, Westlake AA, *et al*. The feasibility of measuring frailty to predict disability and mortality in older medical intensive care unit survivors. *J Crit Care* 2014;29:401–8.
3 Needham DM, Dinglas VD, Morris PE, *et al*. Physical and cognitive performance of patients with acute lung injury 1 year after initial trophic versus full enteral feeding. EDEN trial follow-up. *Am J Respir Crit Care Med* 2013;188:567–76.
4 Wunsch H, Linde-Zwirble WT, Angus DC, *et al*. The epidemiology of mechanical ventilation use in the United States. *Crit Care Med* 2010;38:1947–53.
5 Dinglas VD, Aronson Friedman L, Colantuoni E, *et al*. Muscle weakness and 5-year survival in acute respiratory distress syndrome Survivors*. *Crit Care Med* 2017;45:446–53.
6 Fan E, Dowdy DW, Colantuoni E, *et al*. Physical complications in acute lung injury survivors: a two-year longitudinal prospective study. *Crit Care Med* 2014;42:849–59.
7 Pfoh ER, Wozniak AW, Colantuoni E, *et al*. Physical declines occurring after hospital discharge in ARDS survivors: a 5-year longitudinal study. *Intensive Care Med* 2016;42:1557–66.
8 Desai SV, Law TJ, Needham DM. Long-term complications of critical care. *Crit Care Med* 2011;39:371–9.
9 Puthucheary ZA, Rawal J, McPhail M, *et al*. Acute skeletal muscle wasting in critical illness. *JAMA* 2013;310:1591–600.
10 Puthucheary ZA, Astin R, Mcphail MJW, *et al*. Metabolic phenotype of skeletal muscle in early critical illness. *Thorax* 2018;73:926–35.
11 Files DC, D'Alessio FR, Johnston LF, *et al*. A critical role for muscle ring finger-1 in acute lung injury-associated skeletal muscle wasting. *Am J Respir Crit Care Med* 2012;185:825–34.
12 Bloch SAA, Lee JY, Syburra T, *et al*. Increased expression of GDF-15 may mediate ICU-acquired weakness by down-regulating muscle microRNAs. *Thorax* 2015;70:219–28.
13 Latronico N, Bolton CF. Critical illness polyneuropathy and myopathy: a major cause of muscle weakness and paralysis. *Lancet Neurol* 2011;10:931–41.
14 Fried LP, Ferrucci L, Darer J, *et al*. Untangling the concepts of disability, frailty, and comorbidity: implications for improved targeting and care. *J Gerontol A Biol Sci Med Sci* 2004;59:M255–63.
15 Rockwood K, Song X, MacKnight C, *et al*. A global clinical measure of fitness and frailty in elderly people. *CMAJ* 2005;173:489–95.
16 Muscedere J, Waters B, Varambally A, *et al*. The impact of frailty on intensive care unit outcomes: a systematic review and meta-analysis. *Intensive Care Med* 2017;43:1105–22.
17 Baldwin MR, Singer JP, Huang D, *et al*. Refining low physical activity measurement improves frailty assessment in advanced lung disease and survivors of critical illness. *Ann Am Thorac Soc* 2017;14:1270–9.
18 Calfee CS, Delucchi K, Parsons PE, *et al*. Subphenotypes in acute respiratory distress syndrome: latent class analysis of data from two randomised controlled trials. *Lancet Respir Med* 2014;2:611–20.
19 Famous KR, Delucchi K, Ware LB, *et al*. Acute respiratory distress syndrome subphenotypes respond differently to randomized fluid management strategy. *Am J Respir Crit Care Med* 2017;195:331–8.
20 Rindskopf D, Rindskopf W. The value of latent class analysis in medical diagnosis. *Stat Med* 1986;5:21–7.
21 Rubenfeld GD, Caldwell E, Peabody E, *et al*. Incidence and outcomes of acute lung injury. *N Engl J Med* 2005;353:1685–93.
22 Needham DM, Wozniak AW, Hough CL, *et al*. Risk factors for physical impairment after acute lung injury in a national, multicenter study. *Am J Respir Crit Care Med* 2014;189:1214–24.
23 Herridge MS, Tansey CM, Matté A, *et al*. Functional disability 5 years after acute respiratory distress syndrome. *N Engl J Med* 2011;364:1293–304.
24 Fried LP, Tangen CM, Walston J, *et al*. Frailty in older adults: evidence for a phenotype. *J Gerontol A Biol Sci Med Sci* 2001;56:M146–57.
25 Hlatky MA, Boineau RE, Higginbotham MB, *et al*. A brief self-administered questionnaire to determine functional capacity (the Duke activity status index). *Am J Cardiol* 1989;64:651–4.
26 Taylor HL, Jacobs DR, Schucker B, *et al*. A questionnaire for the assessment of leisure time physical activities. *J Chronic Dis* 1978;31:741–55.
27 Ely EW, Inouye SK, Bernard GR, *et al*. Delirium in mechanically ventilated patients: validity and reliability of the confusion assessment method for the intensive care unit (CAM-ICU). *JAMA* 2001;286:2703–10.
28 Borson S, Scanlan J, Brush M, *et al*. The mini-cog: a cognitive 'vital signs' measure for dementia screening in multi-lingual elderly. *Int J Geriatr Psychiatry* 2000;15:1021–7.
29 Katz S, Ford AB, Moskowitz RW, *et al*. Studies of illness in the aged. The index of ADL: a standardized measure of biological and psychosocial function. *JAMA* 1963;185:914–9.
30 Vermeulen A, Verdonck L, Kaufman JM. A critical evaluation of simple methods for the estimation of free testosterone in serum. *J Clin Endocrinol Metab* 1999;84:3666–72.
31 Holick MF. Vitamin D deficiency. *N Engl J Med* 2007;357:266–81.
32 Cappola AR, Xue Q-L, Fried LP. Multiple Hormonal Deficiencies in Anabolic Hormones Are Found in Frail Older Women: The Women's Health and Aging Studies. *J Gerontol A Biol Sci Med Sci* 2009;64A:243–8.
33 Maggio M, Lauretani F, De Vita F, *et al*. Multiple hormonal dysregulation as determinant of low physical performance and mobility in older persons. *Curr Pharm Des* 2014;20:3119–48.
34 Kennel PJ, Saha A, Maldonado DA, *et al*. Serum exosomal protein profiling for the non-invasive detection of cardiac allograft rejection. *J Heart Lung Transplant* 2018;37:409-417.
35 Ferrante LE, Murphy TE, Leo-Summers LS, *et al*. The combined effects of frailty and cognitive impairment on Post-ICU disability among older ICU survivors. *Am J Respir Crit Care Med* 2019;200:107–10. 1535-4970 (Electronic).

36 Ritchie ME, Phipson B, Wu D, *et al*. limma powers differential expression analyses for RNA-sequencing and microarray studies. *Nucleic Acids Res* 2015;43:e47.
37 Matthews L, Gopinath G, Gillespie M, *et al*. Reactome knowledgebase of human biological pathways and processes. *Nucleic Acids Res* 2009;37:D619–22.
38 Wu D, Smyth GK. Camera: a competitive gene set test accounting for inter-gene correlation. *Nucleic Acids Res* 2012;40:e133.
39 Petersen T. Time-Aggregation bias in Continuous-Time Hazard-Rate models. *Sociol Methodol* 1991;21:263–90.
40 Wurpts IC, Geiser C. Is adding more indicators to a latent class analysis beneficial or detrimental? Results of a Monte-Carlo study. *Front Psychol* 2014;5:920.
41 Kass RE, Raftery AE. Bayes factors. *J Am Stat Assoc* 1995;90:773–95.
42 Nelson JE, Cox CE, Hope AA, *et al*. Chronic critical illness. *Am J Respir Crit Care Med* 2010;182:446–54.
43 Van den Berghe G, de Zegher F, Veldhuis JD, *et al*. The somatotropic axis in critical illness: effect of continuous growth hormone (GH)-releasing hormone and GH-releasing peptide-2 infusion. *J Clin Endocrinol Metab* 1997;82:590–9.
44 Van den Berghe G, de Zegher F, Baxter RC, *et al*. Neuroendocrinology of prolonged critical illness: effects of exogenous thyrotropin-releasing hormone and its combination with growth hormone secretagogues. *J Clin Endocrinol Metab* 1998;83:309–19.
45 Van den Berghe G, Baxter RC, Weekers F, *et al*. The combined administration of GH-releasing peptide-2 (GHRP-2), TRH and GnRH to men with prolonged critical illness evokes superior endocrine and metabolic effects compared to treatment with GHRP-2 alone. *Clin Endocrinol* 2002;56:655–69.
46 Sharshar T, Bastuji-Garin S, Polito A, *et al*. Hormonal status in protracted critical illness and in-hospital mortality. *Crit Care* 2011;15:R47.
47 Griffith DM, Lewis S, Rossi AG, *et al*. Systemic inflammation after critical illness: relationship with physical recovery and exploration of potential mechanisms. *Thorax* 2016;71:820–9.
48 Maddux AB, Hiller TD, Overdier KH, *et al*. Innate immune function and organ failure recovery in adults with sepsis. *J Intensive Care Med* 2019;34:486–94.
49 Stortz JA, Murphy TJ, Raymond SL, *et al*. Evidence for persistent immune suppression in patients who develop chronic critical illness after sepsis. *Shock* 2018;49:249–58.
50 Singer JP, Lederer DJ, Baldwin MR. Frailty in pulmonary and critical care medicine. *Ann Am Thorac Soc* 2016;13:1394–404.
51 Mira JC, Gentile LF, Mathias BJ, *et al*. Sepsis pathophysiology, chronic critical illness, and persistent Inflammation-Immunosuppression and catabolism syndrome. *Crit Care Med* 2017;45:253–62.
52 Yende S, D'Angelo G, Kellum JA, *et al*. Inflammatory markers at hospital discharge predict subsequent mortality after pneumonia and sepsis. *Am J Respir Crit Care Med* 2008;177:1242–7.
53 Leng SX, Xue Q-L, Tian J, *et al*. Inflammation and frailty in older women. *J Am Geriatr Soc* 2007;55:864–71.
54 Cesari M, Penninx BWJH, Pahor M, *et al*. Inflammatory markers and physical performance in older persons: the InCHIANTI study. *J Gerontol A Biol Sci Med Sci* 2004;59:M242–8.
55 Maggio M, Lauretani F, Ceda GP, *et al*. Relationship between low levels of anabolic hormones and 6-year mortality in older men: the aging in the Chianti area (InCHIANTI) study. *Arch Intern Med* 2007;167:2249–54.
56 Cappola AR, Maggio M, Ferrucci L. Is research on hormones and aging finished? No! just started! *J Gerontol A Biol Sci Med Sci* 2008;63:696–8.
57 Nair KS, Rizza RA, O'Brien P, *et al*. DHEA in elderly women and DHEA or testosterone in elderly men. *N Engl J Med* 2006;355:1647–59.
58 Wu FCW, Tajar A, Beynon JM, *et al*. Identification of late-onset hypogonadism in middle-aged and elderly men. *N Engl J Med* 2010;363:123–35.
59 Bidlingmaier M, Friedrich N, Emeny RT, *et al*. Reference intervals for insulin-like growth factor-1 (IGF-I) from birth to senescence: results from a multicenter study using a new automated chemiluminescence IGF-I immunoassay conforming to recent international recommendations. *J Clin Endocrinol Metab* 2014;99:1712–21.
60 Melmed S. Pathogenesis and diagnosis of growth hormone deficiency in adults. *N Engl J Med* 2019;380:2551–62.
61 Woon FL, Dunn CB, Hopkins RO. Predicting cognitive sequelae in survivors of critical illness with cognitive screening tests. *Am J Respir Crit Care Med* 2012;186:333–40.
62 Pandharipande PP, Girard TD, Jackson JC, *et al*. Long-term cognitive impairment after critical illness. *N Engl J Med* 2013;369:1306–16.
63 Pfoh ER, Chan KS, Dinglas VD, *et al*. Cognitive screening among acute respiratory failure survivors: a cross-sectional evaluation of the Mini-Mental state examination. *Critical Care* 2015;19:220.
64 Ahasic AM, Van Ness PH, Murphy TE, *et al*. Functional status after critical illness: agreement between patient and proxy assessments. *Age Ageing* 2015;44:506–10.
65 Covinsky KE, Palmer RM, Counsell SR, *et al*. Functional status before hospitalization in acutely ill older adults: validity and clinical importance of retrospective reports. *J Am Geriatr Soc* 2000;48:164–9.
66 Pol MC, Buurman BM, de Vos R, *et al*. Patient and proxy rating agreements on activities of daily living and the instrumental activities of daily living of acutely hospitalized older adults. *J Am Geriatr Soc* 2011;59:1554–6.
67 Shamsi KS, Pierce A, Ashton AS, *et al*. Proteomic screening of glycoproteins in human plasma for frailty biomarkers. *J Gerontol A Biol Sci Med Sci* 2012;67:853–64.
68 Terrasini N, Lionetti V. Exosomes in critical illness. *Crit Care Med* 2017;45:1054–60.
69 Tanaka T, Biancotto A, Moaddel R, *et al*. Plasma proteomic signature of age in healthy humans. *Aging Cell* 2018;17:e12799.
70 López-Otín C, Blasco MA, Partridge L, *et al*. The hallmarks of aging. *Cell* 2013;153:1194–217.
71 Dos Santos C, Hussain SNA, Mathur S, *et al*. Mechanisms of chronic muscle wasting and dysfunction after an intensive care unit stay. A pilot study. *Am J Respir Crit Care Med* 2016;194:821–30.
72 Jiroutková K, Krajčová A, Ziak J, *et al*. Mitochondrial function in skeletal muscle of patients with protracted critical illness and ICU-acquired weakness. *Crit Care* 2015;19:448.
73 Jackson JC, Ely EW, Morey MC, *et al*. Cognitive and physical rehabilitation of intensive care unit survivors: results of the return randomized controlled pilot investigation. *Crit Care Med* 2012;40:1088–97.

Frailty Subtypes and Recovery in Older Survivors of Acute Respiratory Failure. A Pilot Study.

Matthew R. Baldwin, MD, MS; Lauren R. Pollack, MD; Wendy C. Gonzalez, MD; Richard A. Friedman, PhD; Simone Norris, MS; Alka Javaid, BS; Max R. O'Donnell, MD, MPH; Matthew J. Cummings, MD; Dale Needham, MD, PhD; Elizabeth Colantuoni, PhD; Ursula M. Staudinger, PhD; Mathew S. Maurer, MD; David J. Lederer, MD, MS

SUPPLEMENTARY MATERIAL

TABLE OF CONTENTS

TABLE OF CONTENTS (CONTINUED)

E-METHODS

Enrollment of Participants

Exclusion criteria included: severe dementia based on a Clinical Dementia Rating score of >2.0; lives outside of the United States; undomiciled; does not speak English or Spanish; received lung transplantation; received extracorporeal membrane oxygenation for acute respiratory failure; required emergent cardiothoracic, abdominal, or vascular surgery; had pre-existing neurological injury or disease with motor deficits; respiratory failure due to a primary neurologic diagnosis; no surrogate; planned discharge to hospice at the time of enrollment.

Criteria for Querying the Surrogate

We asked the surrogate questions about the patient's baseline functional status for any patients who lacked capacity to sign informed consent, and in those who had cognitive impairment based on CAM-ICU or Mini-cog testing. If a surrogate was unsure about a patient's activities prior to hospitalization, we asked the surrogate to ask other family members or healthcare aides, or we asked permission from the surrogate to speak with other family members or healthcare aides who spent time with the patient prior to hospitalization. For prospective follow-up measurements of disability, we queried the surrogate who provided informed consent when the patient was not able to provide answers for him/herself.

Table E1. Assessment of Fried frailty phenotype criteria in older survivors of acute respiratory failure

Shrinking (weight loss)	Shrinking was defined as report as an unintentional weight loss of ≥ 10 pounds in the year prior to hospitalization involving intensive care. We asked the surrogate if the participant could not recall. We chose the year prior to hospitalization involving intensive care because weight changes during the index hospitalization may be confounded by treatments for critical illness (e.g. fluid resuscitation for shock, diuresis for pulmonary edema). In the rare instances when the participant and surrogate were unsure, we checked the electronic medical record outpatient notes for participants who received primary care through Columbia University Medical Center, and determined whether the participant lost 10 pounds or more in the year prior to hospitalization based on weights documented at outpatient visits.
Weakness (Decreased grip strength)	Weakness was assessed at the initial assessment during the week prior to hospital discharge while participants were on the general ward since making this measurement in the ICU is often not feasible because most patients are too critically ill to interact. We measured dominant hand grip dynamometry with the JAMAR Plus+ dynamometer (Patterson Medical, Illinois, USA), and calculated the average grip strength of 3 consecutive tests of maximum grip, as was done in the Cardiovascular Health Study (CHS). To assess the traditional frailty phenotype, weakness was defined based on the CHS criteria. Men met the criteria for weakness if their BMI and grip strength were ≤24 kg/m^2 and ≤29 kg; 24.1-26 kg/m^2 and ≤30 kg; 26.1-28 kg/m^2 and ≤31 kg; and >28 kg/m^2 and ≤32 kg, respectively. Women met the criteria for weakness if their BMI and grip strength were ≤23 kg/m^2 and ≤17 kg; 23.1-26 kg/m^2 and ≤17.3kg; 26.1-29 kg/m^2 and ≤18 kg; and >29 kg/m^2 and ≤21 kg, respectively (1).
Slowness (4.57-meter walk speed)	Slowness was assessed at the initial assessment during the week prior to hospital discharge while participants were on the general ward, since making this measurement in the ICU admission is often not feasible because most patients are too critically ill to walk. Participants were allowed up to 3 trials of walking 4.57 meters at a normal pace. We used the fastest walk time as the measurement of slowness. Participants were allowed to use canes or walkers, and those who required supplemental oxygen had their supply carried by a nurse assistant. Slowness was defined based on the CHS methodology. Men met criteria if height and walk time were ≤173 cm and ≥7 seconds, or >173 cm and ≥6 seconds, respectively. Women met criteria if height and walk time were ≤159 cm and ≥7 seconds, or >159 cm and ≥6 seconds,

	respectively.(1) Subjects who were unable to walk 4.57 meters with physical therapy had a gait speed of 0 m/s imputed and were considered slow.
Low Physical Activity	We chose to assess physical activity one month prior to hospitalization for both scientific and practical reasons. From a scientific perspective, in the Cardiovascular Health Study, Fried et al. intended to assess physical function in community-dwelling older adults at their baseline (1). Therefore, there is inherent validity in measuring older ICU survivors' function one month prior to hospitalization, since by doing so we capture these participants' baseline function. We substituted the Duke Activities Status Index for the Minnesota Leisure Time Physical Activity questionnaire, since in our prior work we showed that the DASI improves the construct and predictive validity of frailty assessments in ARF survivors (2). To assess the traditional frailty phenotype, low physical activity was defined based on our previously validated cutoffs (men, ≤12.5 units; women, ≤10 units) (2). We asked the surrogate about physical activity the month prior to hospitalization if the patient could not remember.
Exhaustion	Feelings of exhaustion were assessed at the initial assessment during the week prior to hospital discharge while participants were on the general ward. We chose to measure feelings of exhaustion during the post-ICU acute care period because we hypothesized feelings of fatigue after critical illness would hinder recovery. Furthermore, we felt that trying to remember and quantify subjective feelings prior to critical illness would predispose to recall bias. Exhaustion was defined as answers of 'moderate amount of time' or 'most of the time' to two statements from the modified 10-item Center for Epidemiologic Studies Depression Scale: "I felt everything I did was an effort for the past two days" and "I could not get going for the past two days" (3).

Additional Demographic and Clinical Variable Measurements

FOCIS-specific variables included the Acute Physiology and Chronic Health Evaluation (APACHE) II score, Charlson comorbidity index, type and duration of mechanical ventilation, and admission and discharge location.

Laboratory Measurements

Table E2. Commercial assays used for serum biomarker measurements

Biomarker	Type of Assay	Manufacturer	Manufacturer Location
IL-6	ELISA	R&D Systems	Minneapolis, MN, USA
TNFR1	ELISA	R&D Systems	Minneapolis, MN, USA
IGF-1	IDS-iSYS	Immunodiagnostics Systems	United Kingdom
DHEAs	chemiluminescent immunoassay	Siemens Healthcare Diagnostics	Deerfield, IL, USA
SHBG	chemiluminescent immunoassay	Siemens Healthcare Diagnostics	Deerfield, IL, USA
albumin	colormetic assay	Roche Diagnostics	Indianapolis, IN, USA

Quantitation of Testosterone using Liquid Chromatography-Mass Spectometry at the Columbia CTSA-Biomarker Core lab: The testosterone was extracted from human serum samples using liquid-liquid extraction. LCMS analysis were done using a triple quadrupole Waters Xevo TQ-S (Waters, Milford, MA) equipped with an electrospray ionization source and integrated with a Waters Acquity UPLC. Chromatographic separation was performed on a Waters C18 BEH column (2.1x100mm, 1.7µm, 130Å) with water and acetonitrile containing 0.1% formic acid as mobile phases. The mass spectrometer was operated under multiple reaction monitoring (MRM) mode with positive electrospray ionization and a MRM transition of 289.2>109.1.

Quantitation of 25-hydroxy vitamin D2 and D3 using Liquid Chromatography-Mass Spectometry at the Columbia University CTSA-Biomarker Core lab: 25-hydroxyvitamin D2 and 25-hydroxyvitamin D3 was measured using Ultra Performance Liquid Chromatography-Tandem Mass Spectrometry (LC-MSMS). 25OHD2 and 25OHD3

was extracted from human serum samples using liquid-liquid extraction and measured using a UPLC-MS/MS platform comprising a triple quadrupole Agilent 6410 mass spectrometer (Agilent, Santa Clara, CA) integrated to Agilent UPLC 1290 series. Chromatographic separation was performed by injecting 10uL of the extract onto a Agilent Poroshell 120 EC-C18 column (3.0 x 50mm, 2.7 µm) with water and methanol containing 0.1% formic acid as mobile solvents. The mass spectrometer was operated under multiple reaction monitoring (MRM) mode with positive electrospray ionization. MRM transitions were m/z 413->395 for 25-OH-D2, 401->383 for 25-OH-D3 and 407->389 for d6-25-OH-D3. Calibrators are standardized against the NIST standards.

Rationale for including cognitive impairment as a latent class indicator variable

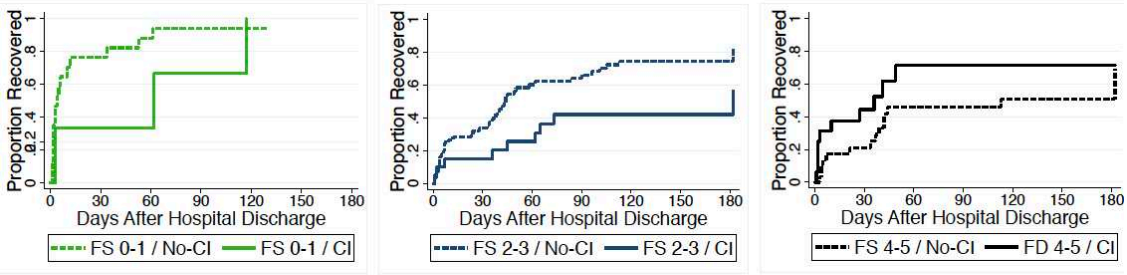

Figure E1. Kaplan Meier plots of recovery to pre-hospitalization Basic ADL function in FOCIS-I participants based on Fried Frailty Index scores using Cardiovascular Health Study criteria (grouped 0-1, 2-3, and 4-5), by the absence vs. presence of Cognitive Impairment (CI) at hospital discharge, p-for-interaction = 0.02. Cognitive impairment was defined as the presence of either delirium, assessed by the Confusion Assessment Method-ICU, or dementia, assessed by the Mini-Cog in those without delirium, during the baseline assessment that occurred on the medical ward during the week prior to hospital discharge.

Rationale for using serum exosomal proteomics

Serum exosomal proteomics is an innovative approach to investigate multisystem dysregulation from a peripheral blood sample (4, 5). Serum proteomics was previously limited because high abundance serum glycoproteins masked lower abundance proteins that may be

novel biomarkers (6-8). Exosomes are 30-100 nm vesicular bodies that are excreted from cells and can enter both neighboring cells and the systemic circulation (9). Exosomes have been recently recognized as a promising noninvasive diagnostic tool in critical illness (10), based on animal and human studies of acute lung injury and sepsis that indicate their involvement in relevant pathobiological functions of vital organs exposed to critical illness stressors (11-14). Protein ontology and pathway analysis of serum exosomal proteomic profiles of ARF survivors offers a systems biology approach to potentially elucidating further the multisystem dysregulation associated with frailty subtypes.

Selection of participants for serum exosome proteomics

Prior to the latent class identification of frailty subtypes, we selected 45 participants for serum exosome proteomics analysis. There were 20 who were not post-ICU frail and 25 who were post-ICU frail by the Fried phenotype criteria. We did not select anyone admitted from a skilled-care facility, and sought to match on age, sex, and pre-hospitalization ADL disability count (Table E4).

Exosome isolation

The Proteomics Shared Resource at Columbia University Medical Center isolated protein from exosomes, performed tandem mass spectroscopy (MS/MS), and identified and quantified exosome proteins.

Exosomes were isolated from 50 µl of participant serum using the Total Exosome Isolation Serum Kit (Invitrogen; ThermoFisher Scientific; Waltham, MA). Total exosome lysate was generated in 50 µl of lysis buffer (50mmlol/liter ammonium bicarbonate, 4 mol/liter urea, and a protease cocktail) using 1.4 mm ceramic beads and a rupture

homogenizer (OmniBead; Omni International, Eugene, OR). Protein concentration in total exosome lysate was determined using the Qubit Protein Assay Kit (Invitrogen; ThermoFisher Scientific; Waltham, MA).

Mass spectroscopy

Fifteen microliters of exosome lysate from each participant was digested by trypsin and labeled with the Amine-Reactive TMT10-plex Isobaric Mass Tag Labeling Regent Set (ThermoFisher Scientific; Waltham, MA) for MS/MS using the Thermo Orbitrap Fusion Tribrid Mass Spectrometer (ThermoFisher Scientific; Waltham, MA). The concentrated peptide mix was reconstituted in a solution of 2% acetonitrile and 2% formic acid for mass spectroscopy analysis. Peptides were loaded with the auto sampler directly on to a 2 cm C18 PepMap pre-column and were eluted from the15cm × 75μm inner diameter PepMap RSLC C18, 3 μm column with a 70-minute gradient from 2% Buffer B to 30% Buffer B (100% acetonitrile and 0.1% formic acid). The gradient was switched from 30% to 85% Buffer B over 5 minutes and held constant for 5 minutes. Finally, the gradient was changed from 85% Buffer B to 98% Buffer A (100% water and 0.1% formic acid) over 1 minute, and then held constant at 98% Buffer A for 8 more minutes. Application of a 2.0 kV distal voltage electrosprayed the eluting peptides directly into the Orbitrap mass spectrometer equipped with an Easy-Spray source (ThermoFinnigan, SanJose,CA). Full mass spectra were recorded on the peptides over a 400-to1,500 m/z range at 120,000 resolution, followed by MS/MS collision-induced dissociation (CID) events for a total cycle of 3 seconds. Charge state-dependent screening was turned off, and peptides with a charge state of 2 to 6 were analyzed.

Mass spectrometer scanning functions and high-performance liquid chromatography gradients were controlled by an Xcalibur data system (ThermoFinnigan, SanJose,CA). Three technical replicates were run for each sample.

Identification of proteins and their concentrations from MS/MS data.

MS/MS data from raw files were searched against FASTA-formatted sequences of the Uniprot human protein database (www.uniprot.org, January 29, 2017) using Proteome Discoverer software v2.2 (ThermoFisher Scientific; Waltham, MA). This application extracts relevant MS/MS spectra from the .raw file and determines the precursor charge state and the quality of the fragmentation spectrum. The software's probability-based score system rates the relevance of the best matches found by the SEQUEST algorithm (15). The peptide search tolerance was set to 10 ppm. A minimum sequence length of 7 amino acid residues was required. Only fully tryptic peptides were considered. To calculate of confidence levels and false discovery rates (FDR), Proteome Discoverer generates a decoy database containing reverse sequences of the non-decoy protein database and performs the search against this concatenated database (non-decoy + decoy) (16). The discriminant score was set at a 5% false discovery rate (FDR). Spectra counts were used as the quantitative values for the protein-based list.

Bioinformatics methods

Analyses were performed with packages in the R/Bioconcutor platform. Intensity values with technical replicates was imputed using the impute package. Qualities were assessed and outliers discarded using Principal Component Analysis (17),

Multidimensional Scaling (18), and Hierarchical clustering (19). All replicates were discarded for a patient containing a single replicate that was an outlier, unless doing so brought the number of patients in a frailty class below 3. After removing outliers, we had 112 samples from 36 patients.

We assessed individual proteome-wide differential protein expression between frailty subtypes using Limma (18), an empirical-Bayesian method (20, 21). The duplicate correlation method, an empirical Bayesian version of mixed-models, was used to include the effect of technical replication in the analysis (22). Given the low sample size and exploratory aim for these proteomic analyses, we set significance at $p < 0.05$ and a FDR < 0.2 and an absolute $\log_2$ fold change of > 0.2.

We conducted the unsupervised clustering analysis using the Cluster 3.0 package (23-25). We calculated the Euclidean distance (24) and performed k-means clustering (24, 26) with k=2 and k=100 iterations. We created heatmaps with protein expression centered using JavaTreeview (23, 27).

We also identified protein functional classes from the Reactome database that differed between frailty subtypes using the Correlation Adjusted Mean Rank gene set test (CAMERA) (28) at $p < 0.05$ and a FDR < 0.2. The pre-ranked mode of CAMERA based on the Limma results was used. We corrected for false discoveries by the method of Benjamini and Hochberg (29). The Reactome database is a peer-reviewed resource of human biological processes functions that can be used to discover functional relationships from expression profile data (30). We then identified those proteins differentially expressed according to Limma which belong to the Reactome protein

functional classes identified by CAMERA in order to identify which proteins may be operative in the differential protein functional classes.

Sensitivity analysis for time-aggregation Bias

The most commonly used time-to-event analyses (i.e. Cox proportional hazards model and Fine and Gray competing risk model) assume that the event of interest can occur along a continuum of time (i.e. time is continuous). However, this assumption that time is exactly or continuously measured is often not met in clinical studies with longitudinal follow-up for survey outcome measures. The limitation with having follow-up at fixed time points is that we cannot observe or realistically ask the participant to recall the exact day during the follow-up interval that she/he regained independence in a specific ADL. Therefore, we assume that the time to recovery is the time to the date of the assessment at which the participant reports having returned to an ADL disability count less than or equal to the pre-hospitalization count. This could result in bias in the effect estimates, called time-aggregation bias (31).

We sought to minimize time-aggregation bias with our fixed time point follow-ups of hospital discharge, and 1-month, 3-month, and 6-month post-hospital discharge follow-up by modeling time-to-recovery and time-to-death as time-in-days rather than discrete-time intervals. Specifically, we chose to model recovery after hospitalization as the time-in-days to the date of the follow-up assessment at which recovery was first achieved, and death after hospitalization as the time-in-days to the date of death, rather than assign a discrete-time interval for recovery or death based on the follow-up at which the event was ascertained (i.e. hospital discharge, 1-month, 3-month, or 6-month follow-up).

Modeling our recovery and death data as time-in-days to event, rather than a discrete-time to event intervals not only minimizes time-aggregation bias, but we believe that it is also the most transparent representation of the data. For example, the time intervals from ICU-discharge to hospital-discharge and hospital discharge to 1-month follow-up varied for participants (median (IQR): 7 (4-12) and 34 (31-42) days, respectively). Therefore, we felt that measuring this time-to-event for those who actually recovered to baseline by hospital discharge or 1 month was more accurately represented as the actual number of days, rather than a time-discrete interval (e.g. “1” for hospital discharge, “2” for 1-month follow-up). As another example, for those who died between the first and third month after hospital discharge, modeling time-to-death as the number of days to the date of death more accurately represents the time they survived rather than a time-discrete interval of “3” for assessing death at the 3-month follow-up visit.

Despite modeling recovery as time-in-days to event, we recognize that we are still assigning recovery times at the end of the appropriate interval of time. Therefore, our results may still be subject to time-aggregation bias. To assess the direction and magnitude of time-aggregation bias in our primary analysis, we conducted a sensitivity analysis that sought to minimize time-aggregation bias when using an estimator that assumes exact measurements of duration (31). For those who achieved recovery, we assigned the midpoint of the time interval between the date of the follow-up assessment at which recovery was ascertained and the date of the previous follow-up assessment at which recovery had not yet been achieved. An example calculation for a single patient who recovered is shown in the figure below.

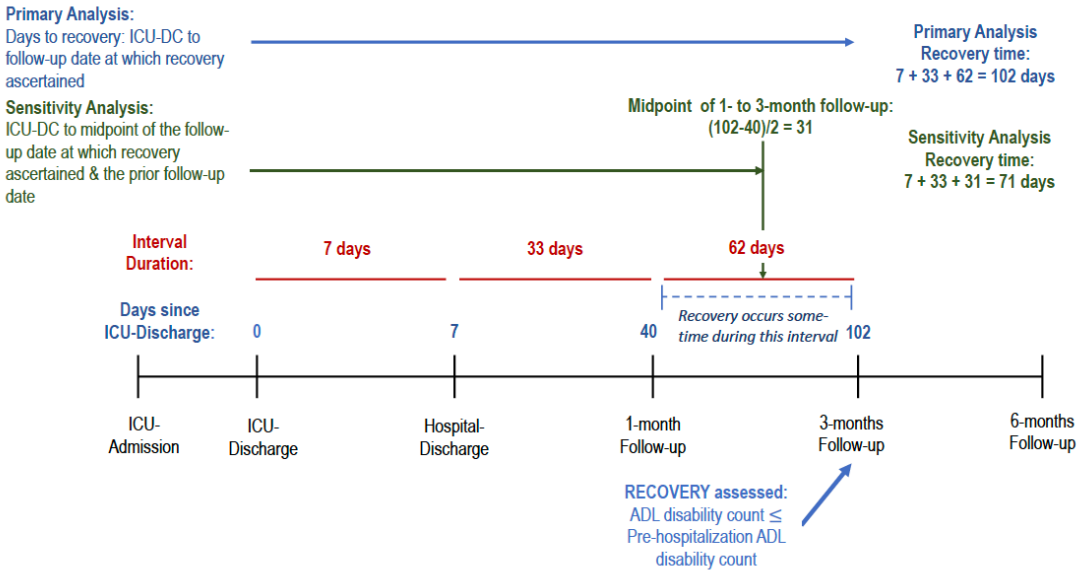

Figure. Example of how recovery time was calculated in the primary analysis versus sensitivity analysis that was done to assess for time aggregation bias due to interval follow-up.

SUPPLEMENT E-RESULTS

Table E3. List of latent class indicator variables included in latent class models.

Variable	Number of patients with data (total n = 185)	Number of patients with missing data	% missing data
Gait-speed	174	11	6.0%
Grip-Strength	180	5	0.54%
Duke Activity Status Index score	181	4	2.7%
Weight loss	182	3	1.6%
Cognitive impairment	176	9	4.9%

Table E4. Cytokine, vitamin D, and hormone levels during the week prior to hospital discharge in FOCIS study participants.

Hormone	IL-6 (pg/ml)	TNFR-1 (pg/ml)	25-hydroxy Vitamin D (ng/ml)	DHEAs (ug/ml)
All, median (IQR); mean (±SD)	12 (6.1-24); 23 (±46)	3193 (2375-5225); 5259 (±5667)	25 (18-32); 25 (±11)	
Men, median (IQR); mean (SD)				0.15 (0.15-0.37); 0.29 (±0.28)
Women, median (IQR); mean (±SD)				0.16 (0.15-0.27); 0.24 (±0.14)

Hormone	Total Testosterone (ng/ml)	Free-Testosterone (pg/ml)	IGF-1 (ng/ml)
All, median (IQR); mean (±SD)			
Men, median (IQR); mean (±SD)	1.68 (0.72-2.53); 1.82 (±1.38)	26.9 (13.3-45.1); 30.7 (±22.2)	61 (38-92); 69 (±43)
Women, median (IQR); mean (±SD)	0.081 (0.05-0.13); 0.12 (±0.17)	1.07 (0.50-1.86); 1.74 (±2.90)	60 (36-92); 69 (±44)

TNFR-1: Tumor necrosis factor soluble receptor 1. IL6: Interleukin-6.
DHEAs: dehydroepiandrosterone-sulfate. IGF-1: Insulin growth factor-1.
Free testosterone was calculated from total testosterone using the Vermeulen formula.

Table E5. Characteristics of n = 45 sub-sample of older acute respiratory failure survivors with serum exosome proteomics by frailty subtype

Characteristic	Subtype 1	Subtype 2	Subtype 3	Subtype 4	Subtype 5	p-value
Number of Subjects	16	9	11	5	4	
Demographics						
Age in years, mean (SD)	71 (10)	71 (6.4)	71 (4.5)	78 (7.8)	77 (5.5)	0.275
Male	7 (44)	3 (33)	5 (46)	2 (40)	2 (50)	0.977
Race						0.93
White	15 (94)	1 (11)	1 (9)	0 (0)	0 (0)	
Black	1 (6)	8 (89)	9 (82)	5 (100)	4 (100)	
Other	0 (0)	0 (0)	1 (9)	0 (0)	0 (0)	
Hispanic Ethnicity	9 (56)	5 (56)	10 (91)	1 (20)	3 (75)	0.073
Pre-hospital variables						
Residence						
Home	15 (100)	9 (100)	13 (100)	4 (100)	4 (100)	<0.001
Skilled-care facility	0 (0)	0 (0)	0 (0)	0 (0)	0 (0)	
ADL dependency count	0	0	0	1 (0-3)	0.5 (0-1)	0.046
Clinical Frailty Scale score	2 (2-2)	4 (-35)	3 (2-5)	5 (4-6)	6 (4-6)	0.001
Charlson Comorbidity Index Score	1 (0.5-2)	2 (1-3)	2 (1-4)	2 (1-5)	4.5 (3.5-5.5)	0.078
ICU variables						
APACHE II Score, mean (SD)	27 (6.3)	29 (11)	35 (8.8)	29 (4.3)	32 (5.4)	0.084
Type of Respiratory Support						0.6
Mechanical Ventilation	14 (88)	8 (89)	11 (100)	4 (80)	4 (100)	
Noninvasive Mechanical Ventilation Only	2 (12)	1 (11)	0 (0)	1 (20)	0 (0)	
ICU days	3 (2-6)	4 (3-6)	8 (7-16)	7 (3-8)	7 (3-13)	0.011
Post-ICU variables						
Post-ICU Frailty Phenotype score	1 (0-2)	3 (1-4)	3 (3-4)	4 (3-4)	3 (3-4)	0.0001
Cognitive Impairment*	2 (13)	1 (11)	5 (46)	0 (0)	4 (100)	0.002
ADL dependency count at hospital discharge	0 (0-2)	1 (0-2)	5 (2-6)	4 (3-5)	6 (6-6)	<0001
Total hospital days	9 (5-15)	11 (7-24)	20 (17-35)	18 (11-31)	17 (13-22)	0.027
Discharge Location						0.001
Home	15 (94)	7 (78)	4 (36)	1 (20)	1 (25)	
Skilled-care facility	1 (6)	2 (22)	7 (64)	4 (80)	3 (75)	
Died in 6 months	0 (0)	0 (0)	4 (36)	1 (20)	1 (33)	<0.001

Data are presented as n(%) or Median (IQR) unless otherwise stated. ADL: Activities of Daily Living. *Cognitive impaired defined as either delirium using the Confusion Assessment Method-ICU or dementia using the Mini-Cog test (score ≤2). Cognitive impairment assessments were conducted during the baseline assessment on the ward, after the ICU, during the week before hospital discharge.

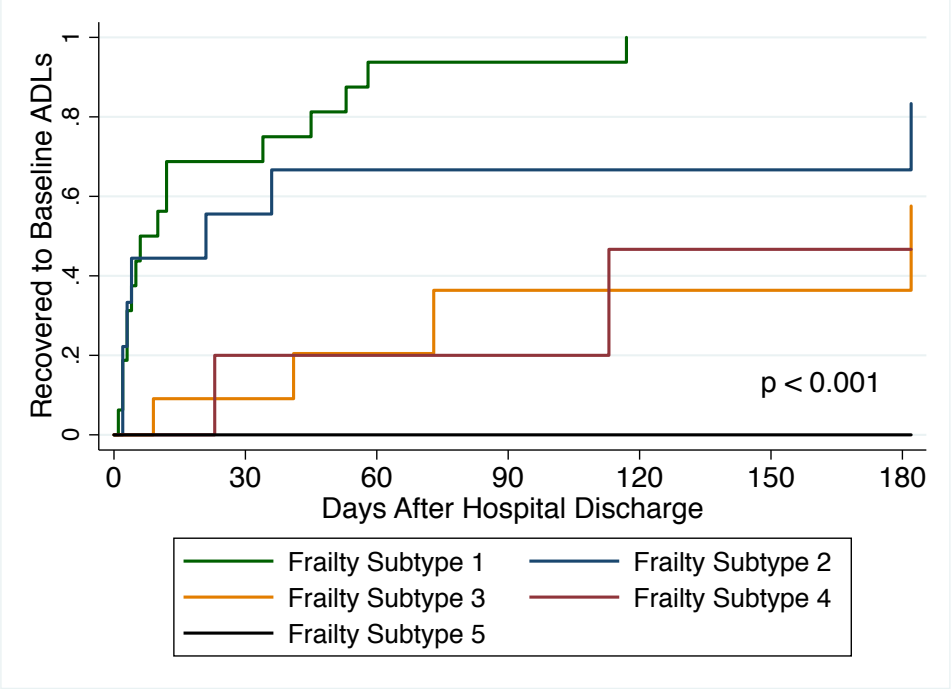

Figure E2. Kaplan-Meier cumulative incidence plots of frailty subtypes showing recovery to pre-hospitalization basic activities of daily living (ADLs) independence within 6-months after hospital discharge for the n = 45 sub-sample with serum exosome proteomics.

Table E6. Frailty subtype 1 serum exosomal differential protein expression and protein functional class regulation (compared to frailty subtype 2)

Exosomal proteome-wide differential protein expression identified with Limma (absolute log fold change >0.2 and FDR < 0.2)			
Count	Protein	Log Fold Change	FDR
1	KRT1	0.647	0.034
2	IGKV2D-24	-0.531	0.034
3	CP	0.257	0.034
4	KRT10	0.665	0.047
5	IGHV4-28	-0.398	0.074
6	A0A0G2JRQ6	-0.946	0.079
Differential Reactome protein functional classes regulation identified with CAMERA (FDR < 0.2)			
Count	Protein Functional Class	Direction of Regulation	FDR
1	**Immune System**		
2	REACTOME_INNATE_IMMUNE_SYSTEM	Down	0.034
5	REACTOME_COMPLEMENT_CASCADE	Down	0.034
3	REACTOME_REGULATION_OF_COMPLEMENT_CASCADE	Down	0.034
4	REACTOME_ACTIVATION_OF_NF_KAPPAB_IN_B_CELLS	Up	0.034
6	REACTOME_DOWNSTREAM_SIGNALING_EVENTS_OF_B_CELL_RECEPTOR_BCR	Up	0.034
7	REACTOME_SIGNALING_BY_THE_B_CELL_RECEPTOR_BCR	Up	0.034
8	REACTOME_CROSS_PRESENTATION_OF_SOLUBLE_EXOGENOUS_ANTIGENS_ENDOSOMES	Up	0.178
9	REACTOME_ANTIGEN_PROCESSING_CROSS_PRESENTATION	Up	0.094
10	REACTOME_ANTIGEN_PROCESSING_UBIQUITINATION_PROTEASOME_DEGRADATION	Up	0.065
11	REACTOME_VIF_MEDIATED_DEGRADATION_OF_APOBEC3G	Up	0.034
12	REACTOME_ER_PHAGOSOME_PATHWAY	Up	0.044
13	REACTOME_HIV_INFECTION	Up	0.063
14	REACTOME_HOST_INTERACTIONS_OF_HIV_FACTORS	Up	0.063
	Cell Cycle Functions		
15	REACTOME_CELL_CYCLE	Up	0.034
16	REACTOME_CELL_CYCLE_MITOTIC	Up	0.034
17	REACTOME_SIGNALING_BY_WNT	Up	0.034
18	REACTOME_CELL_CYCLE_CHECKPOINTS	Up	0.034
19	REACTOME_M_G1_TRANSITION	Up	0.034
20	REACTOME_G1_S_TRANSITION	Up	0.034
21	REACTOME_SYNTHESIS_OF_DNA	Up	0.034
22	REACTOME_MITOTIC_G1_G1_S_PHASES	Up	0.034
23	REACTOME_REGULATION_OF_MITOTIC_CELL_CYCLE	Up	0.034
24	REACTOME_MITOTIC_M_M_G1_PHASES	Up	0.034
25	REACTOME_ASSEMBLY_OF_THE_PRE_REPLICATIVE_COMPLEX	Up	0.034
26	REACTOME_DNA_REPLICATION	Up	0.034
27	REACTOME_MEIOSIS	Up	0.057
28	REACTOME_P53_DEPENDENT_G1_DNA_DAMAGE_RESPONSE	Up	0.034
29	REACTOME_P53_INDEPENDENT_G1_S_DNA_DAMAGE_CHECKPOINT	Up	0.034

30	REACTOME_CYCLIN_E_ASSOCIATED_EVENTS_DURING_G1_S_TRANSITION_	Up	0.034
31	REACTOME_AUTODEGRADATION_OF_THE_E3_UBIQUITIN_LIGASE_COP1	Up	0.034
32	REACTOME_S_PHASE	Up	0.034
33	REACTOME_MEIOTIC_RECOMBINATION	Up	0.081
34	REACTOME_CDK_MEDIATED_PHOSPHORYLATION_AND_REMOVAL_OF_CDC6	Up	0.034
35	REACTOME_CDT1_ASSOCIATION_WITH_THE_CDC6_ORC_ORIGIN_COMPLEX	Up	0.034
36	REACTOME_ORC1_REMOVAL_FROM_CHROMATIN	Up	0.034
37	REACTOME_APC_C_CDH1_MEDIATED_DEGRADATION_OF_CDC20_AND_OTHER_APC_C_CDH1_TARGETED_PROTEINS_IN_LATE_MITOSIS_EARLY_G1	Up	0.034
38	REACTOME_APC_C_CDC20_MEDIATED_DEGRADATION_OF_MITOTIC_PROTEINS	Up	0.034
39	REACTOME_AUTODEGRADATION_OF_CDH1_BY_CDH1_APC_C	Up	0.034
40	REACTOME_SCF_BETA_TRCP_MEDIATED_DEGRADATION_OF_EMI1	Up	0.034
41	REACTOME_SCFSKP2_MEDIATED_DEGRADATION_OF_P27_P21	Up	0.034
	Cellular Regulation and Gene Transcription		
42	REACTOME_REGULATION_OF_APOPTOSIS	Up	0.064
43	REACTOME_METABOLISM_OF_MRNA	Up	0.034
44	REACTOME_REGULATION_OF_MRNA_STABILITY_BY_PROTEINS_THAT_BIND_AU_RICH_ELEMENTS	Up	0.034
45	REACTOME_DESTABILIZATION_OF_MRNA_BY_AUF1_HNRNP_D0	Up	0.034
46	REACTOME_TRANSCRIPTION	Up	0.133
47	REACTOME_RNA_POL_I_RNA_POL_III_AND_MITOCHONDRIAL_TRANSCRIPTION	Up	0.133
48	REACTOME_RNA_POL_I_TRANSCRIPTION	Up	0.133
49	REACTOME_RNA_POL_I_PROMOTER_OPENING	Up	0.133
	Metabolism		
50	REACTOME_METABOLISM_OF_AMINO_ACIDS_AND_DERIVATIVES	Up	0.034
51	REACTOME_REGULATION_OF_ORNITHINE_DECARBOXYLASE_ODC	Up	0.068

Proteins differentially expressed by Limma that belong to Reactome functional protein classes identified by CAMERA

Protein	Protein Functional Class	Direction of Regulation	
KRT1	Innate immune system	Down	

Table E7. Frailty subtype 1 serum exosomal differential protein expression and protein functional class regulation (compared to frailty subtype 3)

Exosomal proteome-wide differential protein expression identified with Limma (absolute log fold change >0.2 and FDR < 0.2)			
Count	Protein	Log Fold Change	FDR
1	TGM4	-0.843	0.022
2	SERPINF2	-0.236	0.049
3	GSN	-0.386	0.056
4	SERPINA3	-0.382	0.056
5	FCGR3A	0.334	0.056
6	PIGR	0.585	0.056
7	CRISP3	-0.463	0.056
8	HRG	-0.318	0.056
9	KRT1	0.522	0.056
10	IGHV4-28	-0.373	0.057
11	SOWAHC	-1.497	0.077
12	FCGBP	0.541	0.077
13	IGFALS	-0.539	0.077
14	IGHV4-30-2	-0.462	0.099
15	SELENOP	-0.267	0.099
16	KRT10	0.536	0.100
17	CLEC3B	-0.309	0.131
18	KRT9	0.477	0.131
19	IGLV1-40	0.497	0.152
Differential Reactome protein functional classes identified with CAMERA (FDR < 0.2)			
Count	Protein Functional Class	Direction of Regulation	FDR
0			all >0.2
Proteins differentially expressed by Limma that belong to Reactome functional protein classes identified by CAMERA			
Protein	Protein Functional Class	Direction of Regulation	
None, because no differential protein functional classes were identified			

Table E8. Frailty subtype 1 serum exosomal differential protein expression and protein functional class regulation (compared to frailty subtype 4)

Exosomal proteome-wide differential protein expression identified with Limma (absolute log fold change >0.2 and FDR < 0.2)			
Count	Protein	Log Fold Change	FDR
1	IGKV4-1	-0.447	0.118
Differential Reactome protein functional classes identified with CAMERA (FDR < 0.2)			
Count	Protein Functional Class	Direction of Regulation	FDR
	Immune System		
1	REACTOME_INITIAL_TRIGGERING_OF_COMPLEMENT	Down	0.123
2	REACTOME_CREATION_OF_C4_AND_C2_ACTIVATORS	Down	0.154
Proteins differentially expressed by Limma that belong to Reactome functional protein classes identified by CAMERA			
Protein	Protein Functional Class	Direction of Regulation	
IGKV4-1	REACTOME_INITIAL_TRIGGERING_OF_COMPLEMENT	Down	
IGKV4-1	REACTOME_CREATION_OF_C4_AND_C2_ACTIVATORS	Down	

Table E9. Frailty subtype 1 serum exosomal differential protein expression and protein functional class regulation (compared to frailty subtype 5)

Exosomal proteome-wide differential protein expression identified with Limma (absolute log fold change >0.2 and FDR < 0.2)			
Count	Protein	Log Fold Change	FDR
1	FETUB	-1.136	0.033
2	TRAJ17	-1.419	0.033
3	MST1	0.588	0.033
4	LCN2	1.201	0.033
5	CRP	1.941	0.040
6	TTR	-0.769	0.065
7	SERPINF2	-0.318	0.065
8	IGLV1-40	0.903	0.065
9	SPRTN	2.210	0.068
10	IGLV2-18	0.993	0.106
11	NDST1	-0.547	0.120
12	C4B	0.611	0.120
13	TF	-0.554	0.120
14	KLKB1	-0.409	0.120
15	HPX	-0.563	0.120
16	IGLV3-10	-0.865	0.122
17	CLU	-0.297	0.122
18	ALB	-0.379	0.123
19	KNG1	-0.312	0.123
20	SELENOP	-0.383	0.134
21	SERPIND1	-0.702	0.138
22	PROC	-0.503	0.154
23	IGKV1D-33	0.752	0.161
24	AMBP	-0.365	0.161
25	AHSG	-0.503	0.177
26	SERPINA4	-0.436	0.177
27	GPX3	-0.562	0.200
28	ECM1	0.482	0.200
29	ORM2	-0.462	0.200
Differential Reactome protein functional classes identified with CAMERA (FDR < 0.2)			
Count	Protein Functional Class	Direction of Regulation	FDR
	Immune System		
1	REACTOME_COMPLEMENT_CASCADE	Down	0.173
2	REACTOME_ADAPTIVE_IMMUNE_SYSTEM	Up	0.173
3	REACTOME_ER_PHAGOSOME_PATHWAY	Up	0.173
4	REACTOME_ANTIGEN_PROCESSING_UBIQUITINATION_PROTEASOME_DEGRADATION	Up	0.173
5	REACTOME_DOWNSTREAM_SIGNALING_EVENTS_OF_B_CELL_RECEPTOR_BCR	Up	0.173
6	REACTOME_ACTIVATION_OF_NF_KAPPAB_IN_B_CELLS	Up	0.173
7	REACTOME_SIGNALING_BY_THE_B_CELL_RECEPTOR_BCR	Up	0.173
8	REACTOME_ANTIGEN_PROCESSING_CROSS_PRESENTATION	Up	0.173

9	REACTOME_CLASS_I_MHC_MEDIATED_ANTIGEN_PROCESSING_PRESENTATION	Up	0.173
10	REACTOME_CYTOKINE_SIGNALING_IN_IMMUNE_SYSTEM	Up	0.173
11	REACTOME_VIF_MEDIATED_DEGRADATION_OF_APOBEC3G	Up	0.173
12	REACTOME_HIV_INFECTION	Up	0.173
13	REACTOME_HOST_INTERACTIONS_OF_HIV_FACTORS	Up	0.173
	Cell Cycle Functions		
14	REACTOME_CELL_CYCLE_MITOTIC	Up	0.173
15	REACTOME_SIGNALING_BY_WNT	Up	0.173
16	REACTOME_ORC1_REMOVAL_FROM_CHROMATIN	Up	0.173
17	REACTOME_CELL_CYCLE	Up	0.173
18	REACTOME_P53_INDEPENDENT_G1_S_DNA_DAMAGE_CHECKPOINT	Up	0.173
19	REACTOME_CDK_MEDIATED_PHOSPHORYLATION_AND_REMOVAL_OF_CDC6	Up	0.173
20	REACTOME_CELL_CYCLE_CHECKPOINTS	Up	0.173
21	REACTOME_CYCLIN_E_ASSOCIATED_EVENTS_DURING_G1_S_TRANSITION_	Up	0.173
22	REACTOME_P53_DEPENDENT_G1_DNA_DAMAGE_RESPONSE	Up	0.173
23	REACTOME_M_G1_TRANSITION	Up	0.173
24	REACTOME_G1_S_TRANSITION	Up	0.173
25	REACTOME_CDT1_ASSOCIATION_WITH_THE_CDC6_ORC_ORIGIN_COMPLEX	Up	0.173
26	REACTOME_SYNTHESIS_OF_DNA	Up	0.173
27	REACTOME_AUTODEGRADATION_OF_THE_E3_UBIQUITIN_LIGASE_COP1	Up	0.173
28	REACTOME_MITOTIC_G1_G1_S_PHASES	Up	0.173
29	REACTOME_REGULATION_OF_MITOTIC_CELL_CYCLE	Up	0.173
30	REACTOME_MITOTIC_M_M_G1_PHASES	Up	0.173
31	REACTOME_ASSEMBLY_OF_THE_PRE_REPLICATIVE_COMPLEX	Up	0.173
32	REACTOME_APC_C_CDH1_MEDIATED_DEGRADATION_OF_CDC20_AND_OTHER_APC_C_CDH1_TARGETED_PROTEINS_IN_LATE_MITOSIS_EARLY_G1	Up	0.173
33	REACTOME_APC_C_CDC20_MEDIATED_DEGRADATION_OF_MITOTIC_PROTEINS	Up	0.173
34	REACTOME_AUTODEGRADATION_OF_CDH1_BY_CDH1_APC_C	Up	0.173
35	REACTOME_SCF_BETA_TRCP_MEDIATED_DEGRADATION_OF_EMI1	Up	0.173
36	REACTOME_S_PHASE	Up	0.173
37	REACTOME_SCFSKP2_MEDIATED_DEGRADATION_OF_P27_P21	Up	0.173
38	REACTOME_DNA_REPLICATION	Up	0.173
	Cellular Regulation and Gene Transcription		
39	REACTOME_METABOLISM_OF_MRNA	Up	0.173
40	REACTOME_METABOLISM_OF_RNA	Up	0.173
41	REACTOME_REGULATION_OF_MRNA_STABILITY_BY_PROTEINS_THAT_BIND_AU_RICH_ELEMENTS	Up	0.173
42	REACTOME_MEMBRANE_TRAFFICKING	Up	0.173

43	REACTOME_DESTABILIZATION_OF_MRNA_BY_AUF1_HNRNP_D0	Up	0.173
44	REACTOME_TRANS_GOLGI_NETWORK_VESICLE_BUDDING	Up	0.173
45	REACTOME_GOLGI_ASSOCIATED_VESICLE_BIOGENESIS	Up	0.173
	Metabolism		
46	REACTOME_REGULATION_OF_INSULIN_LIKE_GROWTH_FACTOR_IGF_ACTIVITY_BY_INSULIN_LIKE_GROWTH_FACTOR_BINDING_PROTEINS_IGFBPS	Down	0.173
47	REACTOME_REGULATION_OF_ORNITHINE_DECARBOXYLASE_ODC	Up	0.186
48	REACTOME_PTM_GAMMA_CARBOXYLATION_HYPUSINE_FORMATION_AND_ARYLSULFATASE_ACTIVATION	Down	0.173
49	REACTOME_GAMMA_CARBOXYLATION_TRANSPORT_AND_AMINO_TERMINAL_CLEAVAGE_OF_PROTEINS	Down	0.173

Proteins differentially expressed by Limma that belong to Reactome functional protein classes identified by CAMERA

Protein	Protein Functional Class	Direction of Regulation	
CLU	COMPLEMENT_CASCADE	Down	
CRP	COMPLEMENT_CASCADE	Down	
C4B	COMPLEMENT_CASCADE	Down	
LCN2	CYTOKINE_SIGNALING_IN_IMMUNE_SYSTEM	Up	
TF	MEMBRANE_TRAFFICKING	Up	

Table E10. Frailty subtype 2 serum exosomal differential protein expression and protein functional class regulation (compared to frailty subtype 3)

Exosomal proteome-wide differential protein expression identified with Limma (absolute log fold change >0.2 and FDR < 0.2)			
Count	Protein	Log Fold Change	FDR
1	PIGR	0.910817949	0.01931
2	FCGR2C	0.606356196	0.03191
3	CFHR4	-0.84133022	0.03191
4	HP	-1.230259491	0.05021
5	C9	-0.428717542	0.05993
Differential Reactome protein functional classes identified with CAMERA (FDR < 0.2)			
Count	Protein Functional Class	Direction of Regulation	FDR
0			all >0.2
Proteins differentially expressed by Limma that belong to Reactome functional protein classes identified by CAMERA			
Protein	Protein Functional Class	Direction of Regulation	
None, because no differential protein functional classes were identified			

Table E11. Frailty subtype 2 serum exosomal differential protein expression and protein functional class regulation (compared to frailty subtype 4)

Exosomal proteome-wide differential protein expression identified with Limma (absolute log fold change >0.2 and FDR < 0.2)			
Count	Protein	Log Fold Change	FDR
1	IGLV2-8	0.853430894	0.014
2	CP	-0.374654389	0.0195
3	VCL	0.720239874	0.0384
4	IGHV4-30-2	0.712998347	0.1187
Differential Reactome protein functional classes identified with CAMERA (FDR < 0.2)			
Count	Protein Functional Class	Direction of Regulation	FDR
0			all >0.2
Proteins differentially expressed by Limma that belong to Reactome functional protein classes identified by CAMERA			
Protein	Protein Functional Class	Direction of Regulation	
None, because no differential protein functional classes were identified			

Table E12. Frailty subtype 2 serum exosomal differential protein expression and protein functional class regulation (compared to frailty subtype 5)

Exosomal proteome-wide differential protein expression identified with Limma (absolute log fold change >0.2 and FDR < 0.2)			
Count	Protein	Log Fold Change	FDR
1	FETUB	-1.23286714	0.02667
2	LCN2	1.155408382	0.07211
3	AMBP	-0.469067214	0.1238
4	IGKV1D-33	0.864572367	0.14815
5	TGFBI	0.513221366	0.14815
6	IGLV2-18	1.153498669	0.14815
7	KLKB1	-0.44994892	0.14815
8	MST1	0.540726476	0.17023
9	IGKV1D-13	-2.267569247	0.17023
10	HPX	-0.700607707	0.17023
11	KNG1	-0.331515205	0.17023
12	IGHG4	1.485238115	0.17023
13	ITIH1	-0.415246292	0.17023
14	SERPINF2	-0.277060068	0.17023
15	PROZ	-1.102493098	0.17023
16	SERPIND1	-0.726648749	0.17023
17	SPRTN	1.754369604	0.20069
Differential Reactome protein functional classes identified with CAMERA (FDR < 0.2)			
Count	Protein Functional Class	Direction of Regulation	FDR
1	REACTOME_PTM_GAMMA_CARBOXYLATION_HYPUSINE_FORMATION_AND_ARYLSULFATASE_ACTIVATION	Down	0.0857
2	REACTOME_GAMMA_CARBOXYLATION_TRANSPORT_AND_AMINO_TERMINAL_CLEAVAGE_OF_PROTEINS	Down	0.0857
Proteins differentially expressed by Limma that belong to Reactome functional protein classes identified by CAMERA			
Protein	Protein Functional Class	Direction of Regulation	
PROZ	REACTOME_PTM_GAMMA_CARBOXYLATION_HYPUSINE_FORMATION_AND_ARYLSULFATASE_ACTIVATION	Down	
PROZ	REACTOME_GAMMA_CARBOXYLATION_TRANSPORT_AND_AMINO_TERMINAL_CLEAVAGE_OF_PROTEINS	Down	

Table E13. Frailty subtype 3 serum exosomal differential protein expression and protein functional class regulation (compared to frailty subtype 4)

Exosomal proteome-wide differential protein expression identified with Limma (absolute log fold change >0.2 and FDR < 0.2)			
Count	Protein	Log Fold Change	FDR
1	IGKV4-1	-0.4950067	0.02571
2	IGHV4-30-2	0.72774176	0.12816
3	SAA2-SAA4	1.06600823	0.12816
4	SAA1	1.83720225	0.12816
5	F13A1	-0.504736	0.14899
Differential Reactome protein functional classes identified with CAMERA (FDR < 0.2)			
Count	Protein Functional Class	Direction of Regulation	FDR
0			all >0.2
Proteins differentially expressed by Limma that belong to Reactome functional protein classes identified by CAMERA			
Protein	Protein Functional Class	Direction of Regulation	
None, because no differential protein functional classes were identified			

Table E14. Frailty subtype 3 serum exosomal differential protein expression and protein functional class regulation (compared to frailty subtype 5)

Exosomal proteome-wide differential protein expression identified with Limma (absolute log fold change >0.2 and FDR < 0.2)			
Count	Protein	Log Fold Change	FDR
1	IGLV3-10	-1.1356051	0.07302
2	FCGR3A	-0.5584034	0.07302
3	LCN2	1.10816193	0.07302
4	AHSG	-0.636413	0.12307
5	SPRTN	2.07023074	0.12307
Differential Reactome protein functional classes identified with CAMERA (FDR < 0.2)			
Count	Protein Functional Class	Direction of Regulation	FDR
0			all >0.2
Proteins differentially expressed by Limma that belong to Reactome functional protein classes identified by CAMERA			
Protein	Protein Functional Class	Direction of Regulation	
None, because no differential protein functional classes were identified			

There were no differentially expressed proteins nor Reactome protein functional classes comparing subtype 4 to subtype 5.

SUPPLEMENT REFERENCES

1. Fried LP, Tangen CM, Walston J, Newman AB, Hirsch C, Gottdiener J, Seeman T, Tracy R, Kop WJ, Burke G, McBurnie MA. Frailty in older adults: Evidence for a phenotype. *J Gerontol A Biol Sci Med Sci* 2001; 56A: M146-M156.

2. Baldwin MR, Singer JP, Huang D, Sell J, Gonzalez WC, Pollack LR, Maurer MS, D'Ovidio FF, Bacchetta M, Sonett JR, Arcasoy SM, Shah L, Robbins H, Hays SR, Kukreja J, Greenland JR, Shah RJ, Leard L, Morrell M, Gries C, Katz PP, Christie JD, Diamond JM, Lederer DJ. Refining Low Physical Activity Measurement Improves Frailty Assessment in Advanced Lung Disease and Survivors of Critical Illness. *Annals of the American Thoracic Society* 2017; 14: 1270-1279.

3. Orme JG, Reis J, Herz EJ. Factorial and discriminant validity of the Center for Epidemiological Studies Depression (CES-D) scale. *Journal of clinical psychology* 1986; 42: 28-33.

4. Raimondo F, Morosi L, Chinello C, Magni F, Pitto M. Advances in membranous vesicle and exosome proteomics improving biological understanding and biomarker discovery. *Proteomics* 2011; 11: 709-720.

5. Greening DW, Xu R, Gopal SK, Rai A, Simpson RJ. Proteomic insights into extracellular vesicle biology - defining exosomes and shed microvesicles. *Expert review of proteomics* 2017; 14: 69-95.

6. States DJ, Omenn GS, Blackwell TW, Fermin D, Eng J, Speicher DW, Hanash SM. Challenges in deriving high-confidence protein identifications from data gathered by a HUPO plasma proteome collaborative study. *Nature biotechnology* 2006; 24: 333-338.

7. Anderson NL, Anderson NG. The human plasma proteome: history, character, and diagnostic prospects. *Molecular & cellular proteomics : MCP* 2002; 1: 845-867.

8. Schiess R, Wollscheid B, Aebersold R. Targeted proteomic strategy for clinical biomarker discovery. *Molecular oncology* 2009; 3: 33-44.

9. Yanez-Mo M, Siljander PR, Andreu Z, Zavec AB, Borras FE, Buzas EI, Buzas K, Casal E, Cappello F, Carvalho J, Colas E, Cordeiro-da Silva A, Fais S, Falcon-Perez JM, Ghobrial IM, Giebel B, Gimona M, Graner M, Gursel I, Gursel M, Heegaard NH, Hendrix A, Kierulf P, Kokubun K, Kosanovic M, Kralj-Iglic V, Kramer-Albers EM, Laitinen S, Lasser C, Lener T, Ligeti E, Line A, Lipps G, Llorente A, Lotvall J, Mancek-Keber M, Marcilla A, Mittelbrunn M, Nazarenko I, Nolte-'t Hoen EN, Nyman TA, O'Driscoll L, Olivan M, Oliveira C, Pallinger E, Del Portillo HA, Reventos J, Rigau M, Rohde E, Sammar M, Sanchez-Madrid F, Santarem N, Schallmoser K, Ostenfeld MS, Stoorvogel W, Stukelj R, Van der Grein SG, Vasconcelos MH, Wauben MH, De Wever O. Biological properties of extracellular vesicles and their physiological functions. *Journal of extracellular vesicles* 2015; 4: 27066.

10. Terrasini N, Lionetti V. Exosomes in Critical Illness. *Crit Care Med* 2017; 45: 1054-1060.

11. Wu SC, Yang JC, Rau CS, Chen YC, Lu TH, Lin MW, Tzeng SL, Wu YC, Wu CJ, Hsieh CH. Profiling circulating microRNA expression in experimental sepsis using cecal ligation and puncture. *PloS one* 2013; 8: e77936.

12. Moon HG, Cao Y, Yang J, Lee JH, Choi HS, Jin Y. Lung epithelial cell-derived extracellular vesicles activate macrophage-mediated inflammatory responses via ROCK1 pathway. *Cell death & disease* 2015; 6: e2016.

13. Janiszewski M, Do Carmo AO, Pedro MA, Silva E, Knobel E, Laurindo FR. Platelet-derived exosomes of septic individuals possess proapoptotic NAD(P)H oxidase activity: A novel vascular redox pathway. *Critical care medicine* 2004; 32: 818-825.

14. Kovach MA, Singer BH, Newstead MW, Zeng X, Moore TA, White ES, Kunkel SL, Peters-Golden M, Standiford TJ. IL-36gamma is secreted in microparticles and exosomes by lung macrophages in response to bacteria and bacterial components. *Journal of leukocyte biology* 2016; 100: 413-421.

15. Yates JR, 3rd, Eng JK, McCormack AL, Schieltz D. Method to correlate tandem mass spectra of modified peptides to amino acid sequences in the protein database. *Analytical chemistry* 1995; 67: 1426-1436.

16. Elias JE, Gygi SP. Target-decoy search strategy for increased confidence in large-scale protein identifications by mass spectrometry. *Nature methods* 2007; 4: 207-214.

17. McDonald JW. affycoretools: Functions useful for those doing repetitive analyses with Affymetrix GeneChips. 1.52.2 ed; 2018.

18. Ritchie ME, Phipson B, Wu D, Hu Y, Law CW, Shi W, Smyth GK. limma powers differential expression analyses for RNA-sequencing and microarray studies. *Nucleic acids research* 2015; 43: e47.

19. R Core Team. R: A Language and Environment for Statistical Computing}. 3.5.2 ed. Vienna, Austria: R Foundation for Statistical Computing; 2018.

20. Smyth GK. Linear Models and Empirical Bayes Methods for Assessing Differential Expression in Microarray Experiments. *Statistical Applications in Genetics and Molecular Biology* 2004; 3: Article 3, http://www.bepress.com/sagmb/vol3/iss1/art3/.

21. Ritchie ME, Diyagama D, Neilson J, van Laar R, Dobrovic A, Holloway A, Smyth GK. Empirical array quality weights in the analysis of microarray data. *BMC bioinformatics* 2006; 7: 261.

22. Smyth GK, Michaud J, Scott HS. Use of within-array replicate spots for assessing differential expression in microarray experiments. *Bioinformatics* 2005; 21: 2067-2075.

23. Eisen MB, Spellman PT, Brown PO, Botstein D. Cluster analysis and display of genome-wide expression patterns. *Proc Natl Acad Sci USA* 1998; 95: 14863-14868.

24. Everitt BS, Landau S, Leese M. Cluster Analysis. Wiley; 2011.

25. de Hoon MJ, Imoto S, Nolan J, Miyano S. Open source clustering software. *Bioinformatics* 2004; 20: 1453-1454.

26. Lloyd SP. Least square quantization in PCM. *IEEE Transactions on Information Theory* 1957; 28: 129–137.

27. Saldanha AJ. Java Treeview--extensible visualization of microarray data. *Bioinformatics* 2004; 20: 3246-3248.

28. Wu D, Smyth GK. Camera: a competitive gene set test accounting for inter-gene correlation. *Nucleic acids research* 2012; 40: e133.

29. Benjamini Y, Hochberg Y. Controlling the false discovery rate; A practical and powerful approach to multiple testing. *J Roy Stat Soc Ser B* 1995; 57: 289-300.

30. Matthews L, Gopinath G, Gillespie M, Caudy M, Croft D, de Bono B, Garapati P, Hemish J, Hermjakob H, Jassal B, Kanapin A, Lewis S, Mahajan S, May B, Schmidt E, Vastrik I, Wu G, Birney E, Stein L, D'Eustachio P. Reactome knowledgebase of human biological pathways and processes. *Nucleic acids research* 2009; 37: D619-622.

31. Petersen T. Time-Aggregation Bias in Continuous-Time Hazard-Rate Models. *Sociological Methodology* 1991; 21: 263-290.